Quarkonia and open heavy flavour production in pp, pPb and Pb-Pb collisions with ALICE

Seminaire du

Laboratoire de Physique Corpusculaire

Lizardo Valencia Palomo

17/01/2014

Content

Physics motivation

The ALICE experiment

Open heavy flavours

Quarkonia

Upgrades

Conclusions

The ALICE collaboration

PHYSICS MOTIVATION

Open heavy flavours in heavy-ion collisions

- Ultrarelativistic heavy-ion (HI) collisions → high energy densities.
- Quark Gluon Plasma (QGP): deconfined state of quarks and gluons.

Open heavy flavours in heavy-ion collisions

- Ultrarelativistic heavy-ion (HI) collisions → high energy densities.
- Quark Gluon Plasma (QGP): deconfined state of quarks and gluons.

τ_{QGP} very small
direct observation
not possible!

Open heavy flavours in heavy-ion collisions

- Ultrarelativistic heavy-ion (HI) collisions → high energy densities.
- Quark Gluon Plasma (QGP): deconfined state of quarks and gluons.

τ_{QGP} very small
direct observation
not possible!

Heavy flavours (HF) experience the whole evolution of the system.

Can be used to understand the in-medium partonic energy loss in the QCD matter created in heavy-ion collisions.

QCD & gluon radiation suppression (dead cone effect):

$$\Delta E_g > \Delta E_c > \Delta E_b$$

$$\Rightarrow \quad R_{AA}^{\pi} < R_{AA}^{D} < R_{AA}^{B}$$

NPA 783 (2007) 493, PLB 519 (2001) 199, PRD 71 (2005) 054027

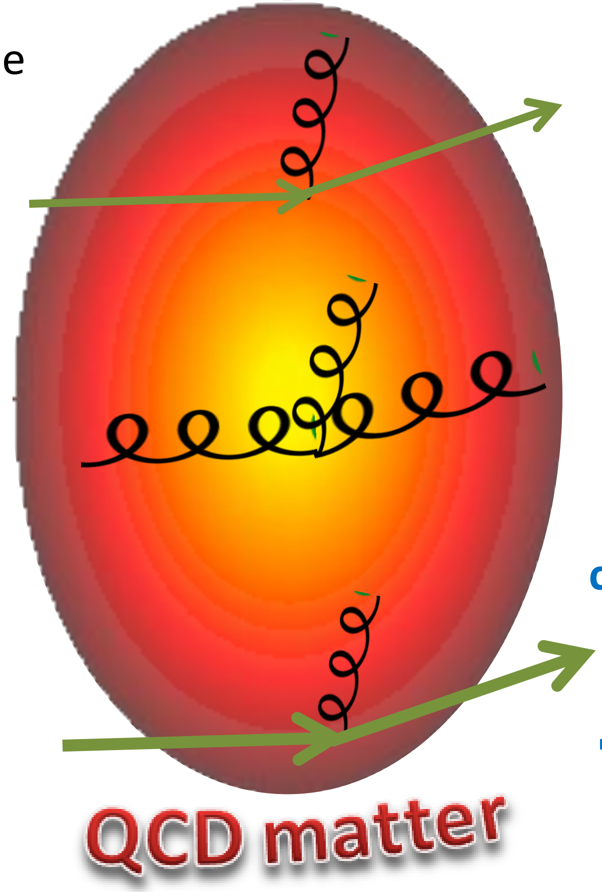

Light quarks:
$m \sim 0$, $C_R = 4/3$
Energy loss

Gluons:
$m = 0$, $C_R = 3$
Larger energy loss

c: $m \sim 1.5$ GeV, $C_R = 4/3$
b: $m \sim 5$ GeV, $C_R = 4/3$
dead cone effect
→ Smaller energy loss

Quarkonia in heavy-ion collisions

- In 1980’s quarkonia is proposed as a probe of the QGP (PLB 178 (1986) 416):
  - ❑ Produced in the early stages of the collisions.
  - ❑ Suppressed by the Debye screening.

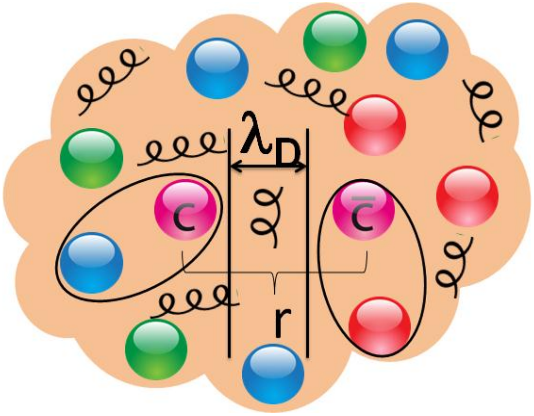

Quarkonia in heavy-ion collisions

- In 1980's quarkonia is proposed as a probe of the QGP (PLB 178 (1986) 416):
  - ❑ Produced in the early stages of the collisions.
  - ❑ Suppressed by the Debye screening.
- Suppression depends on the binding energy of quarkonia states (PRD 64 (2001) 094015):
  - ❑ Excited states melt down at different temperatures ➔ sequential suppression.

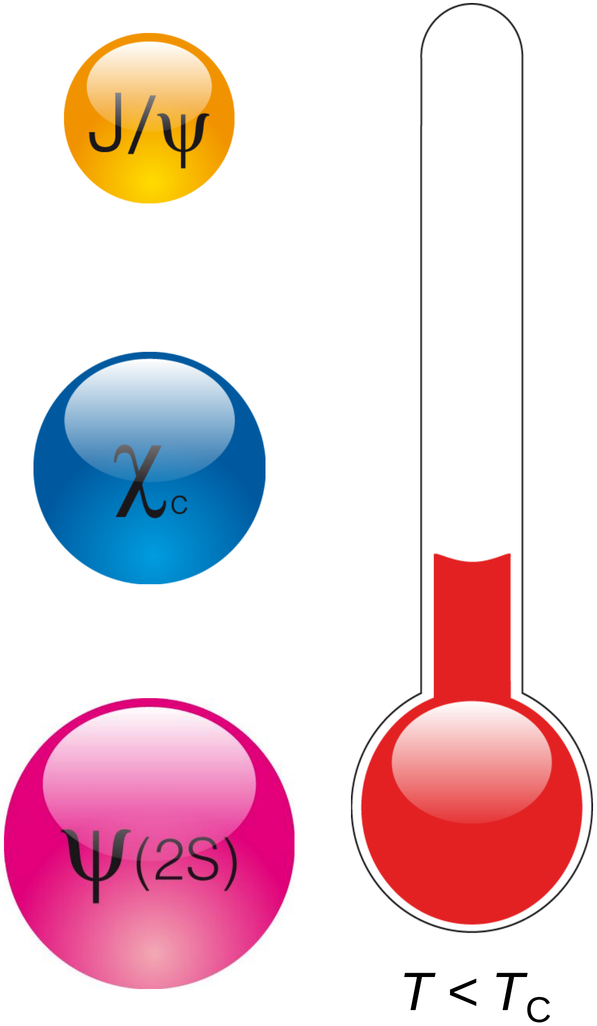

Quarkonia in heavy-ion collisions

- In 1980's quarkonia is proposed as a probe of the QGP (PLB 178 (1986) 416):
  - ❑ Produced in the early stages of the collisions.
  - ❑ Suppressed by the Debye screening.
- Suppression depends on the binding energy of quarkonia states (PRD 64 (2001) 094015):
  - ❑ Excited states melt down at different temperatures ➔ sequential suppression.

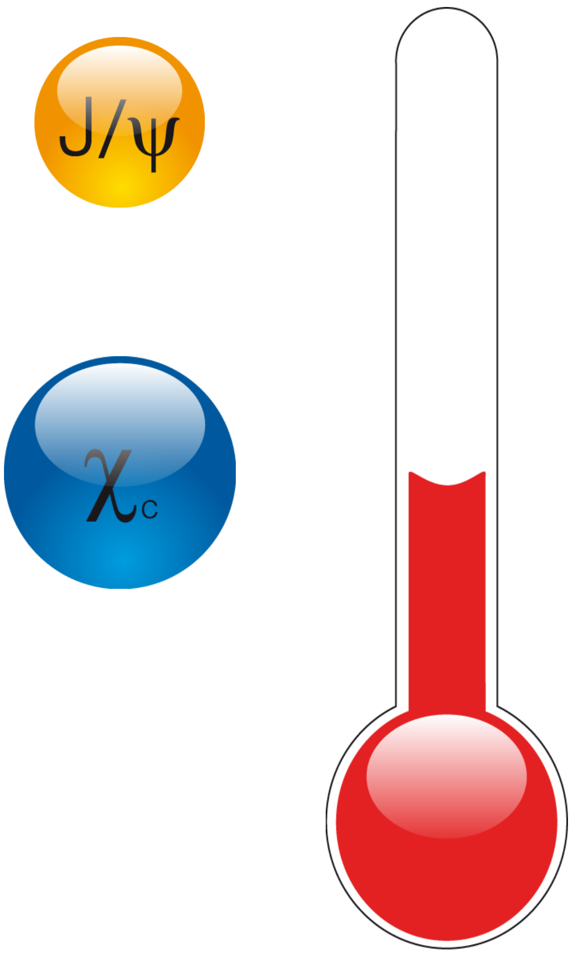

$T \approx T_C$

Quarkonia in heavy-ion collisions

- In 1980's quarkonia is proposed as a probe of the QGP (PLB 178 (1986) 416):
  - ❑ Produced in the early stages of the collisions.
  - ❑ Suppressed by the Debye screening.
- Suppression depends on the binding energy of quarkonia states (PRD 64 (2001) 094015):
  - ❑ Excited states melt down at different temperatures → sequential suppression.

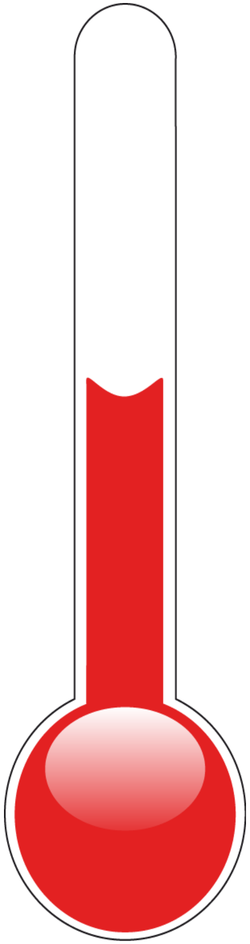

$T \approx 1.1\ T_C$

Quarkonia in heavy-ion collisions

- In 1980's quarkonia is proposed as a probe of the QGP (PLB 178 (1986) 416):
  - ❑ Produced in the early stages of the collisions.
  - ❑ Suppressed by the Debye screening.
- Suppression depends on the binding energy of quarkonia states (PRD 64 (2001) 094015):
  - ❑ Excited states melt down at different temperatures ➔ sequential suppression.
  - ❑ Quarkonia family as a thermometer of the QGP!

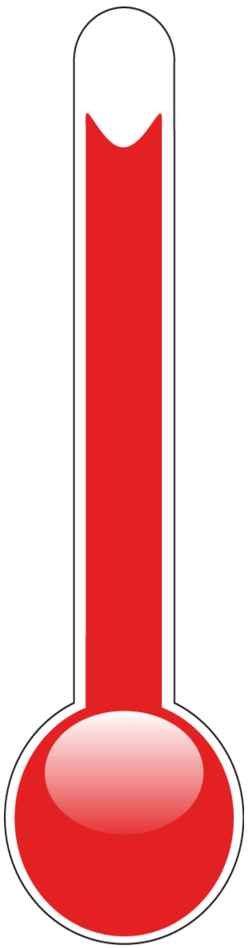

$T \approx 2.1\ T_C$

Quarkonia in heavy-ion collisions

- In 1980's quarkonia is proposed as a probe of the QGP (PLB 178 (1986) 416):
  - ❑ Produced in the early stages of the collisions.
  - ❑ Suppressed by the Debye screening.

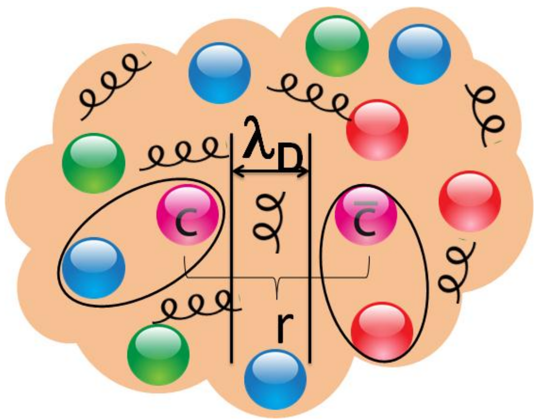

- Suppression depends on the binding energy of quarkonia states (PRD 64 (2001) 094015):
  - ❑ Excited states melt down at different temperatures ➔ sequential suppression.
  - ❑ Quarkonia family as a thermometer of the QGP!

- Charmonia production at the LHC:
  - ❑ $N_{c\bar{c}}$/central collision ≈ 120.

  ➔ new source of J/ψ production from recombination of $c\bar{c}$ pairs?

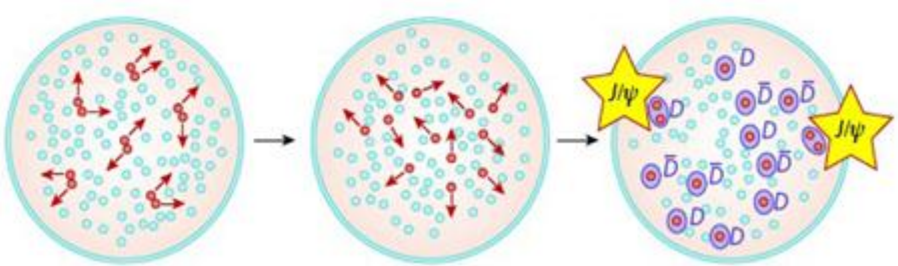

Nature 448 (2007) 302

HF in proton-proton and proton-nucleus collisions

- proton-proton (pp) collisions:
  - ❑ Test pQCD calculations.
  - ❑ Reference for HI studies.

$$R_{\mathrm{AA}} = \frac{d^2N_{\mathrm{AA}}/dp_{\mathrm{T}}d\eta}{\langle N_{\mathrm{coll}}\rangle \; d^2N_{\mathrm{pp}}/dp_{\mathrm{T}}d\eta}$$

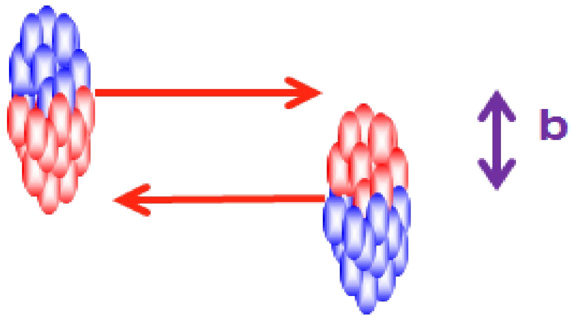

Spectators
Participants
impact parameter

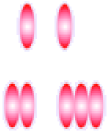

	$N_{part} = 2$	$N_{coll} = 1$
	$N_{part} = 5$	$N_{coll} = 6$
Pb-Pb cent.	$N_{part} = 360$	$N_{coll} = 1500$
p-Pb cent.	$N_{part} = 16$	$N_{coll} = 15$

HF in proton-proton and proton-nucleus collisions

- proton-proton (pp) collisions:
  - ❑ Test pQCD calculations.
  - ❑ Reference for HI studies.
- proton-nucleus (pA) collisions:
  - ❑ Disentangle hot and Cold Nuclear Matter (CNM) effects, intermidiate step between A-A and pp collisions.
  - ❑ Even if the QGP is not created, particle production can be affected by initial/final state effects:
    - ○ Shadowing (JP G32 (2006) R367): gluon PDF of nucleons embedded in nucleus ≠ gluon PDF of free nucleons.
    - ○ Comovers (PRL 77 (1996) 1703): dissocation by other particles produced during the collision.

$$R_{AA} = \frac{d^2N_{AA}/dp_T d\eta}{\langle N_{coll}\rangle \; d^2N_{pp}/dp_T d\eta}$$

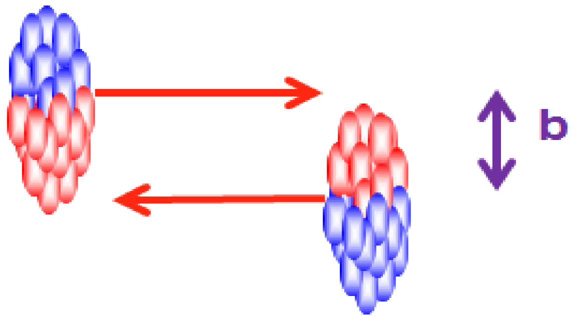

Spectators
Participants
impact parameter

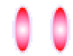	$N_{part} = 2$	$N_{coll} = 1$
	$N_{part} = 5$	$N_{coll} = 6$
Pb-Pb cent.	$N_{part} = 360$	$N_{coll} = 1500$
p-Pb cent.	$N_{part} = 16$	$N_{coll} = 15$

THE ALICE EXPERIMENT

The ALICE experiment

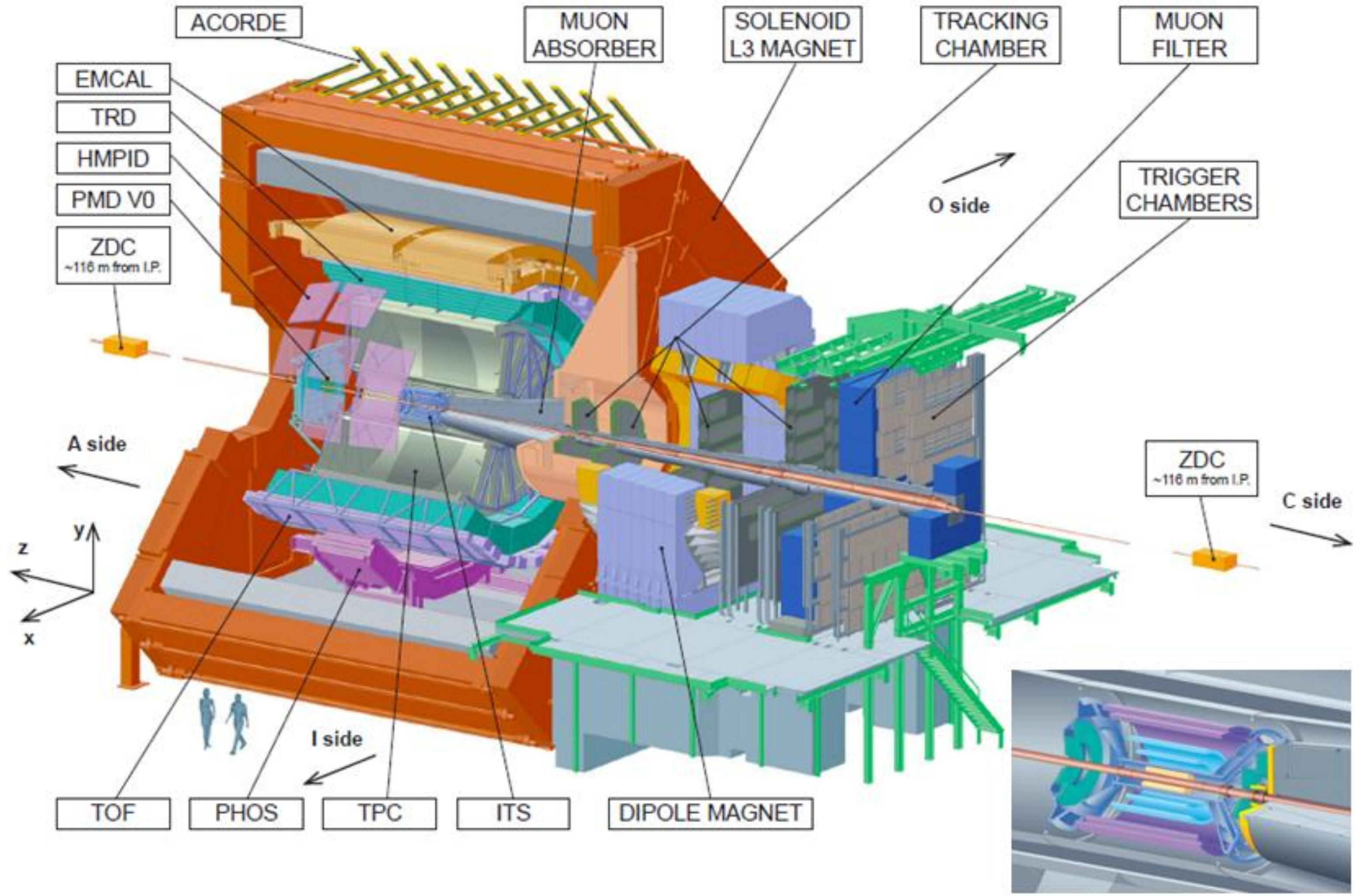

The ALICE experiment

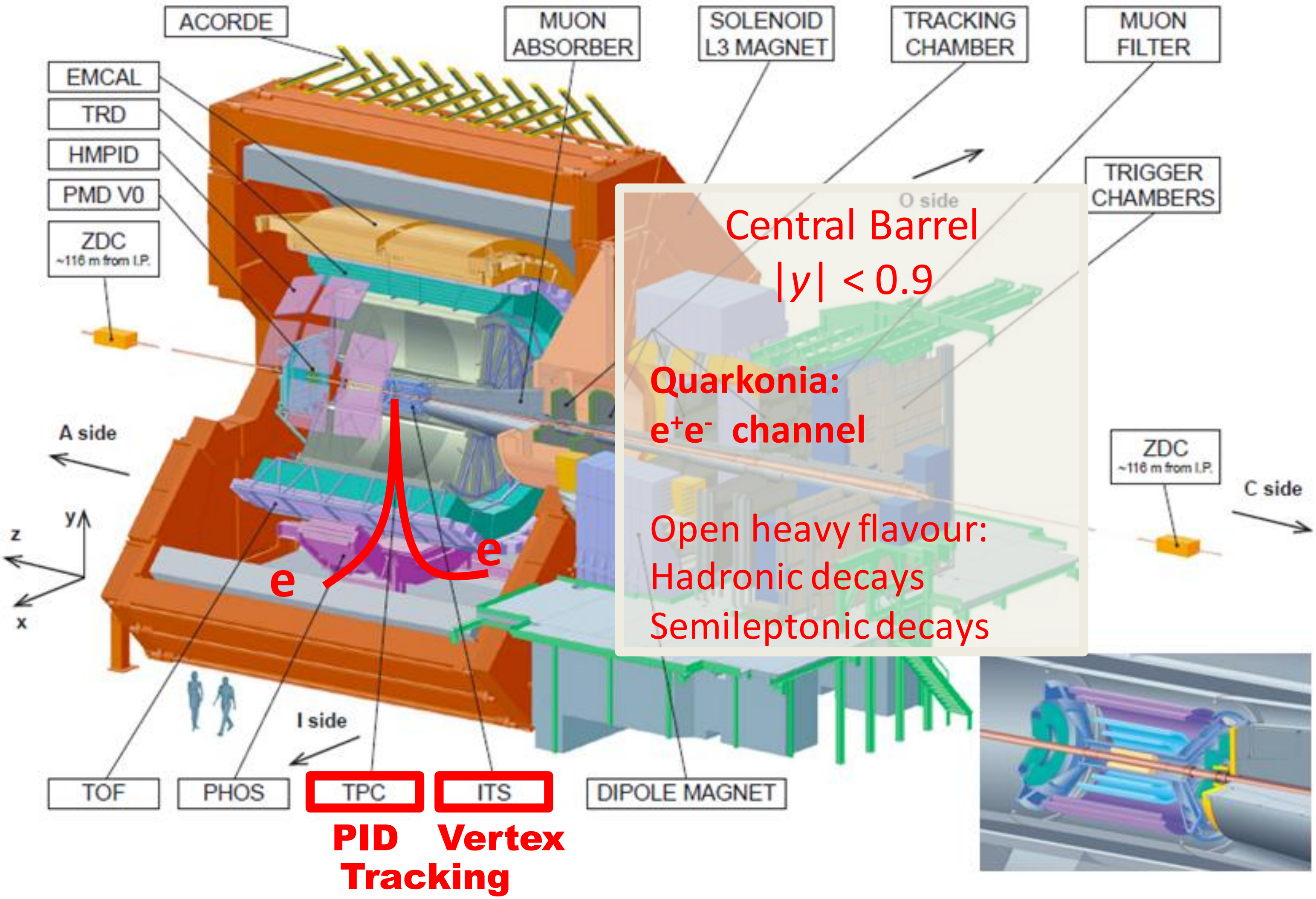

Central Barrel
$|y| < 0.9$

Quarkonia:
$e^{+}e^{-}$ channel

Open heavy flavour:
Hadronic decays
Semileptonic decays

The ALICE experiment

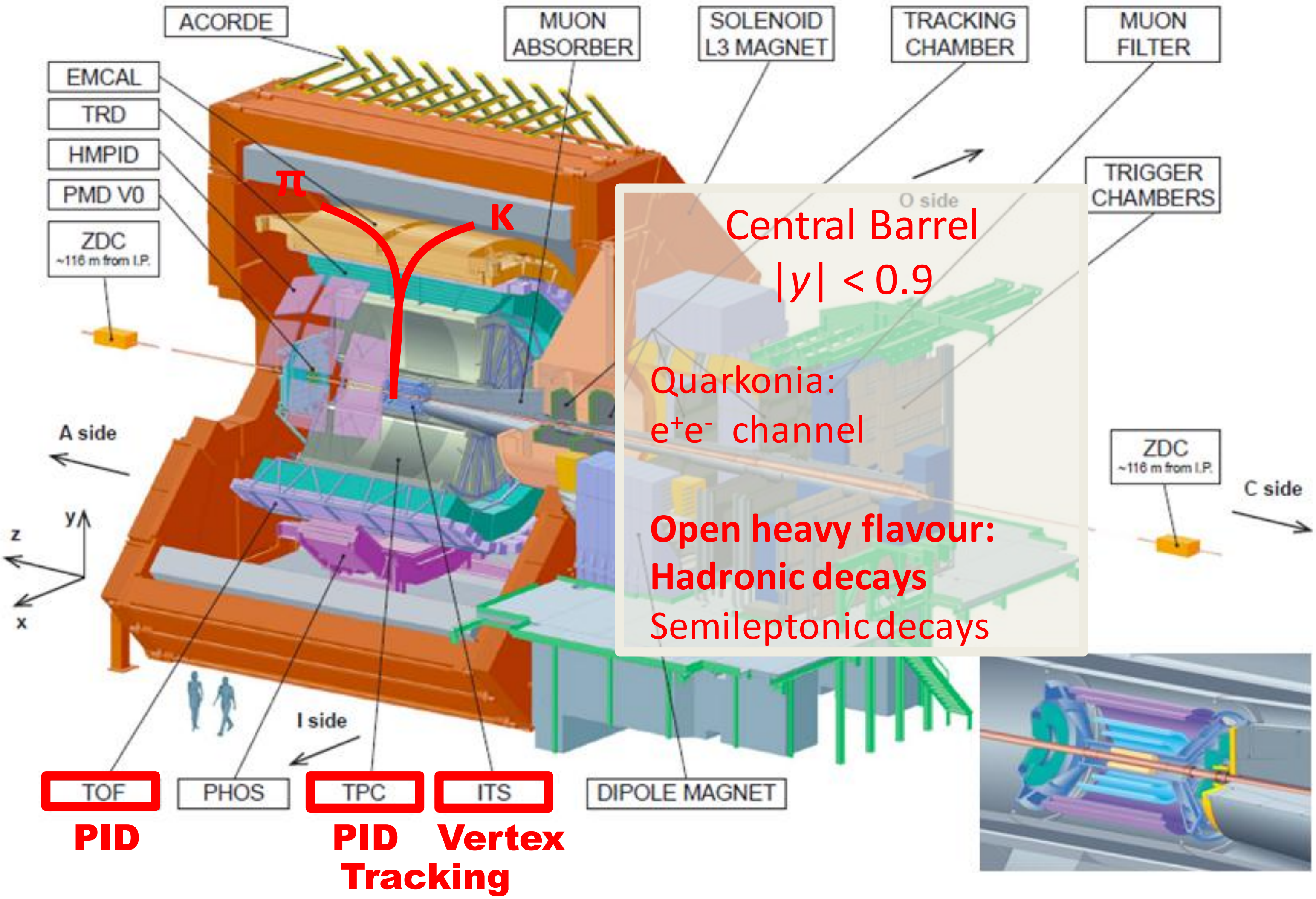

Central Barrel
$|y| < 0.9$

Quarkonia:
e^+e^- channel

Open heavy flavour:
Hadronic decays
Semileptonic decays

The ALICE experiment

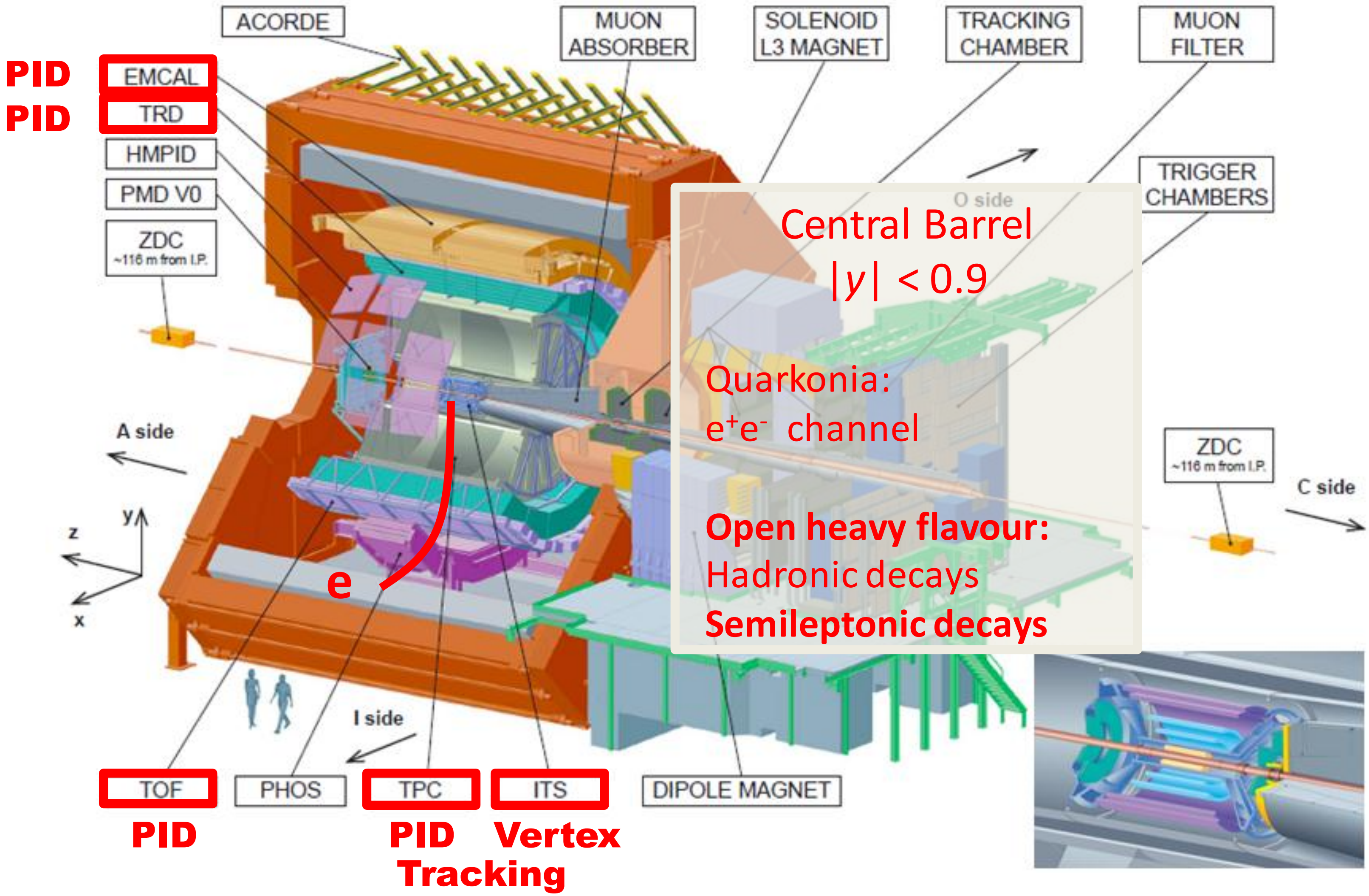

Central Barrel
$|y| < 0.9$

Quarkonia:
e^+e^- channel

Open heavy flavour:
Hadronic decays
Semileptonic decays

The ALICE experiment

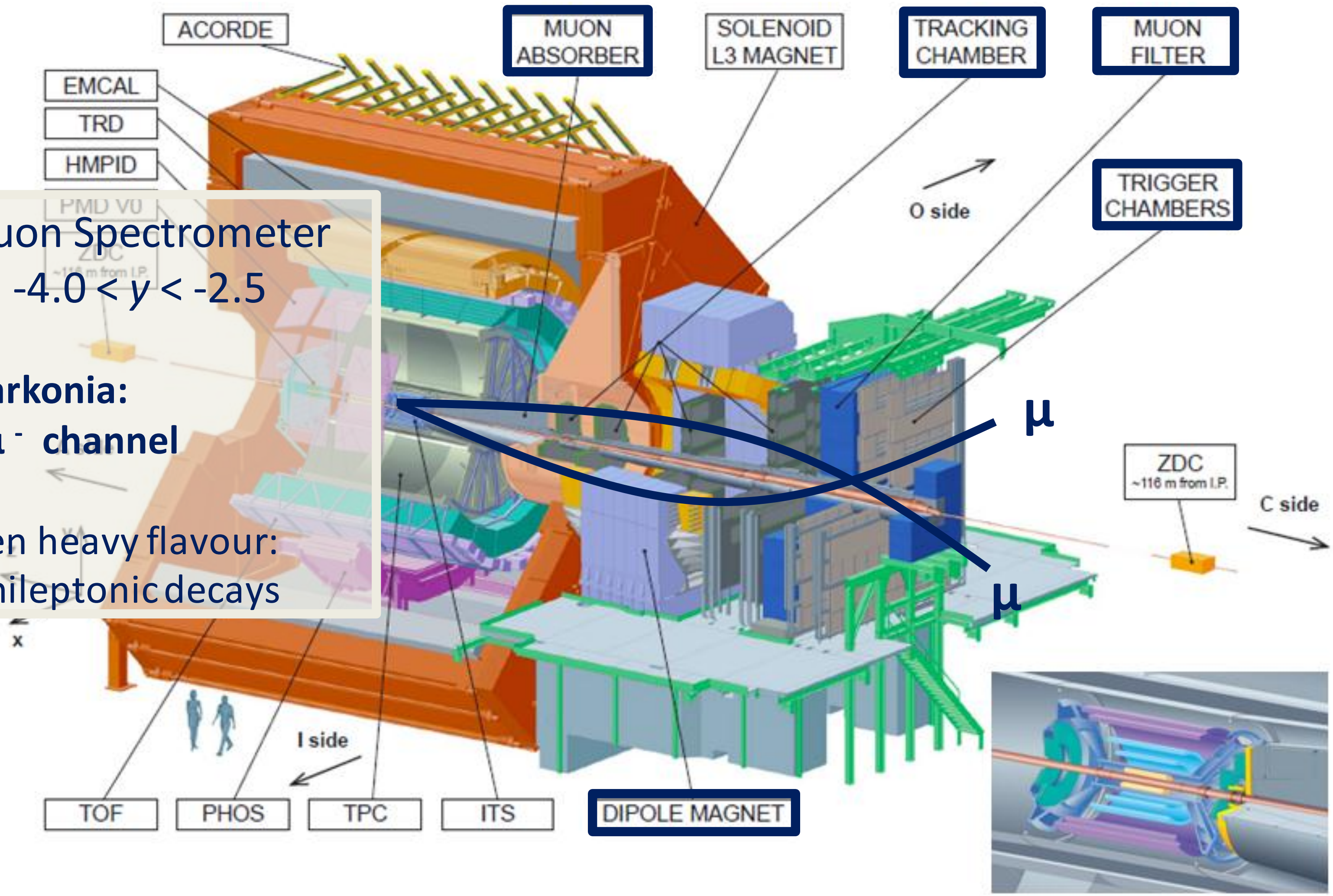

Muon Spectrometer
$-4.0 < y < -2.5$

Quarkonia:
$\mu^+ \mu^-$ channel

Open heavy flavour:
Semileptonic decays

The ALICE experiment

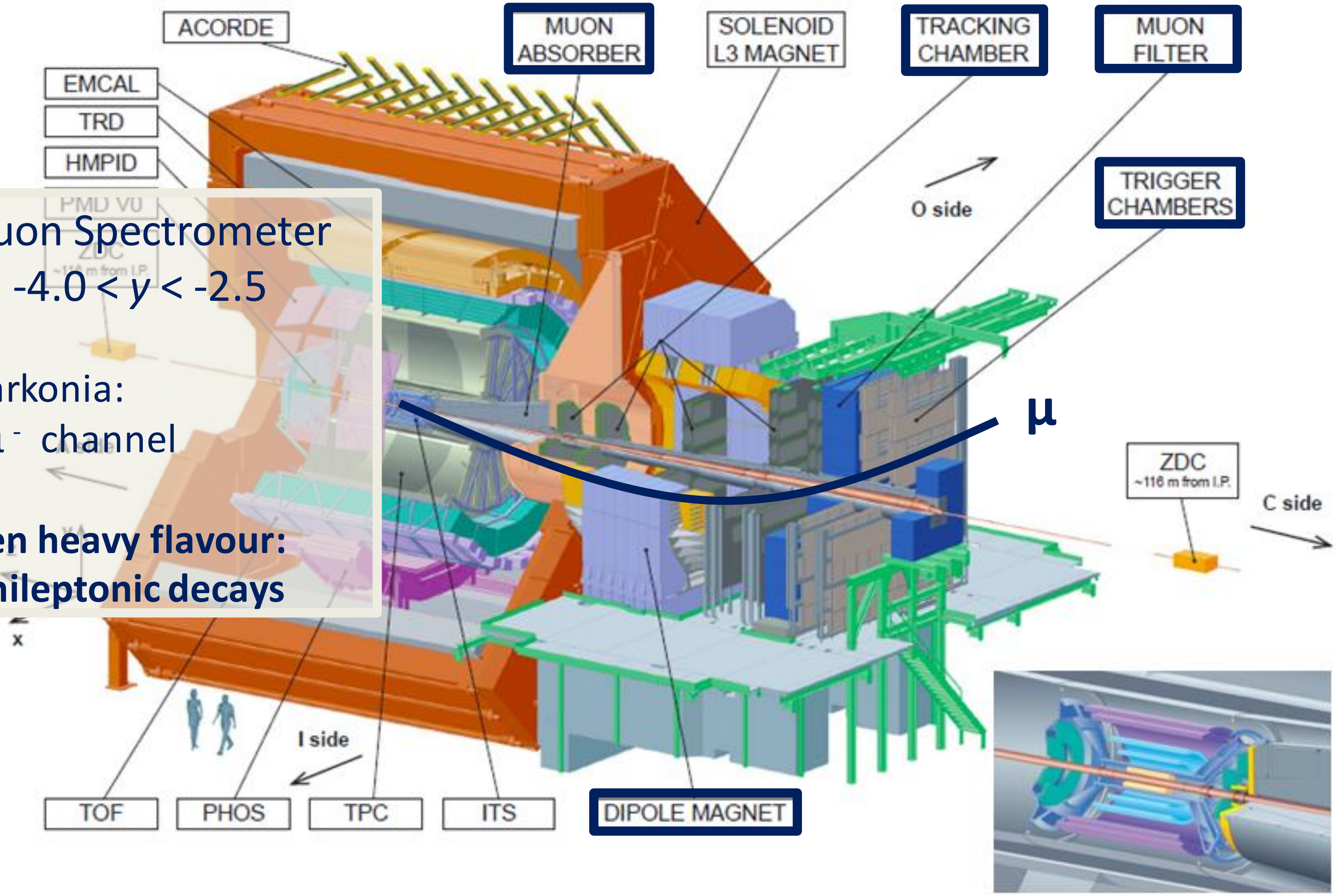

Muon Spectrometer
$-4.0 < y < -2.5$

Quarkonia:
$\mu^+ \mu^-$ channel

Open heavy flavour:
Semileptonic decays

OPEN HEAVY FLAVOURS

ALICE performance

Open heavy flavours {
Precise tracking and vertexing.
Good particle identification.

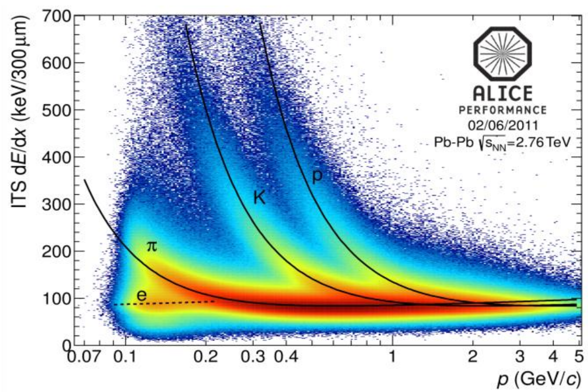

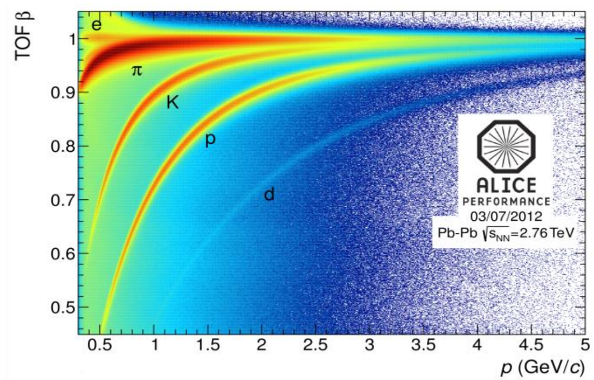

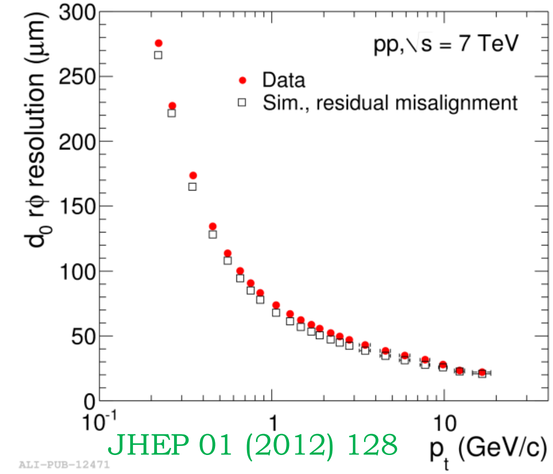

JHEP 01 (2012) 128

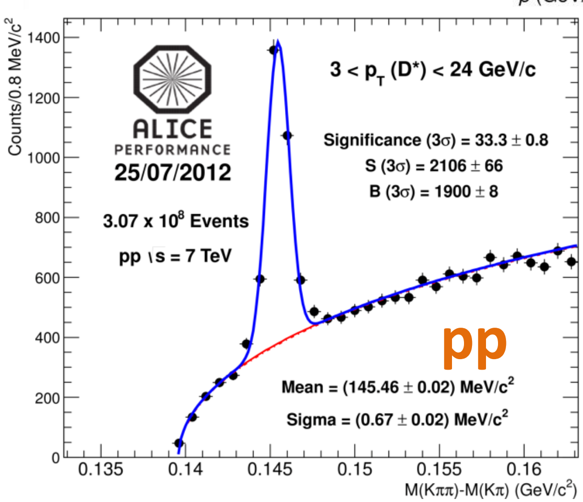

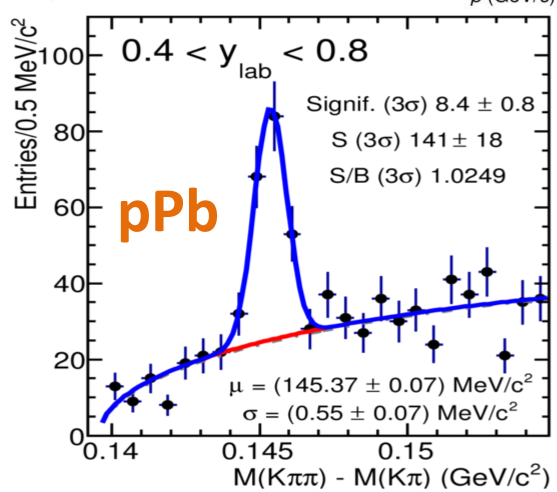

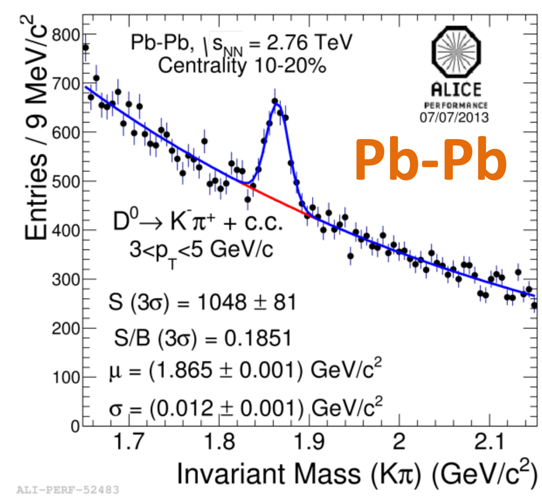

D mesons in pp

Prompt D mesons $d\sigma/p_T$ distributions at 7 and 2.76 TeV are described within uncertainties by pQCD calculations (FONLL & GM-VFNS).

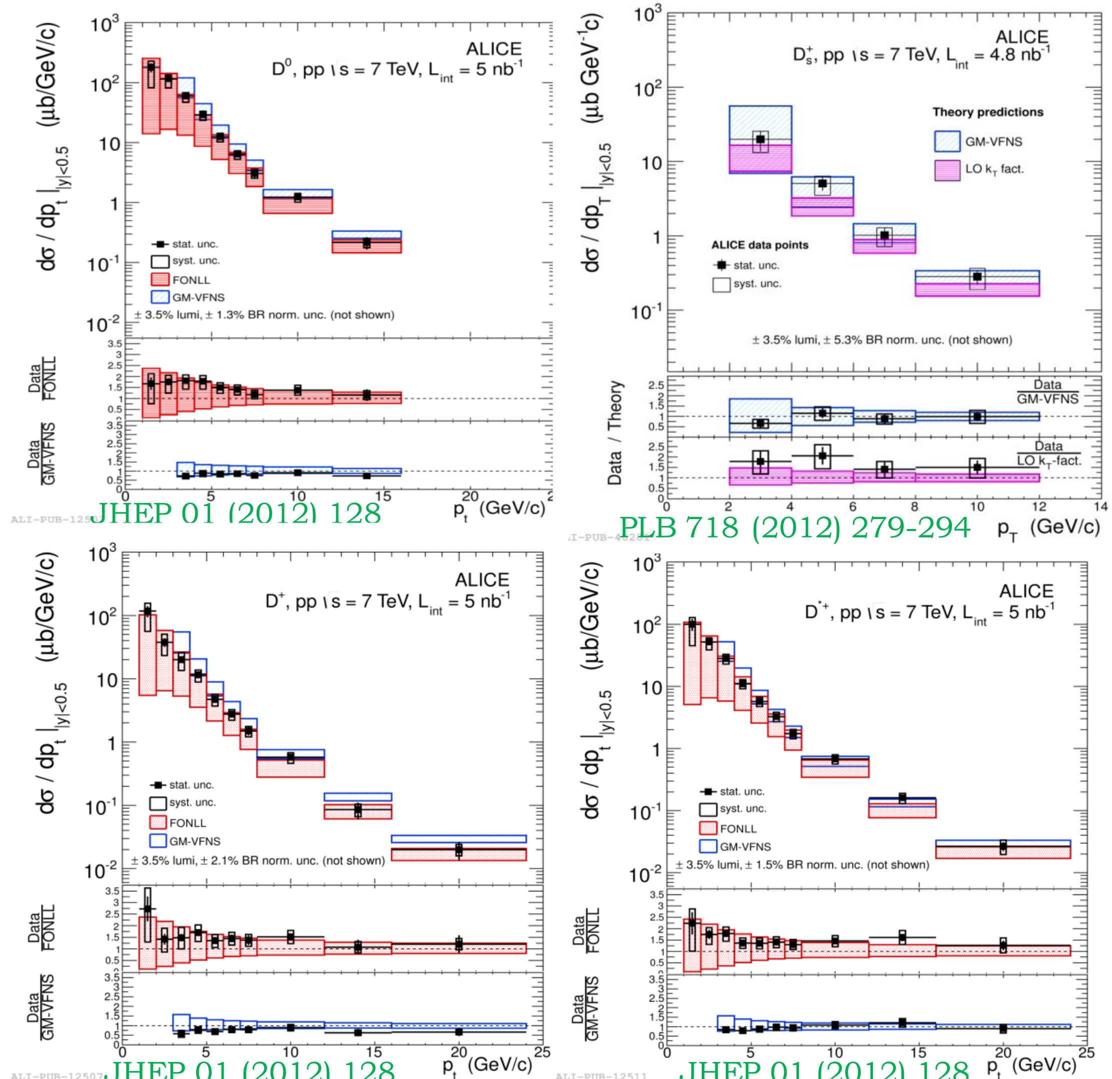

D mesons in pp

Prompt D mesons $d\sigma/p_T$ distributions at 7 and 2.76 TeV are described within uncertainties by pQCD calculations (FONLL & GM-VFNS).

JHEP 1207 (2012) 191

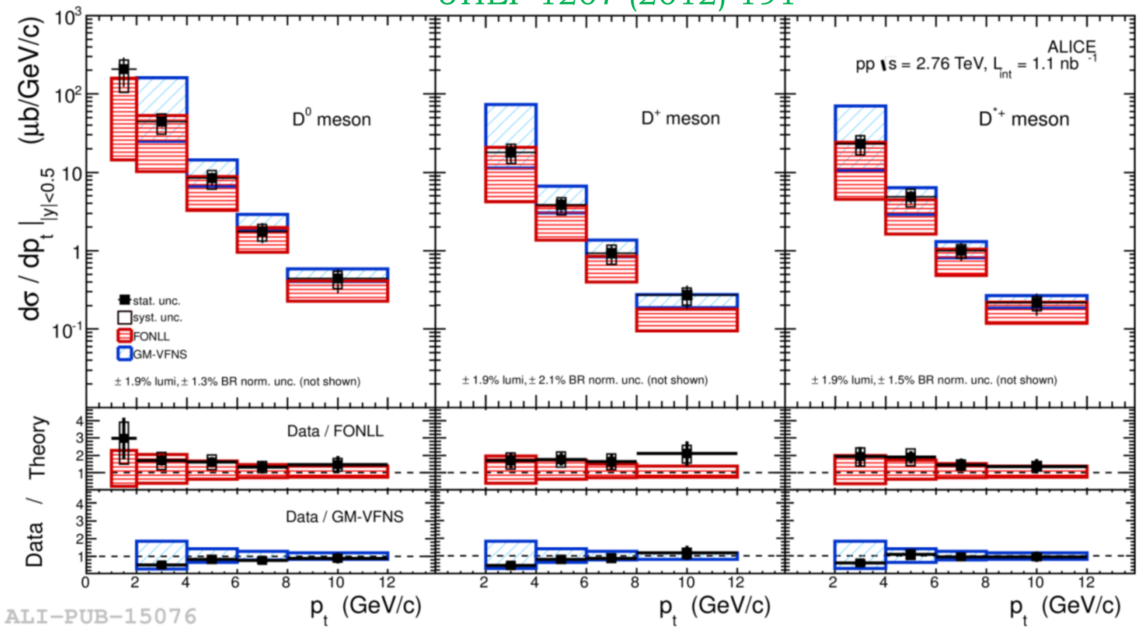

D mesons in pp

Prompt D mesons $d\sigma/p_T$ distributions at 7 and 2.76 TeV are described within uncertainties by pQCD calculations (FONLL & GM-VFNS).

Measured cross-sections extrapolated to full phase space using FONLL scaling factors.

ALICE results in good agreement with other LHC experiments.

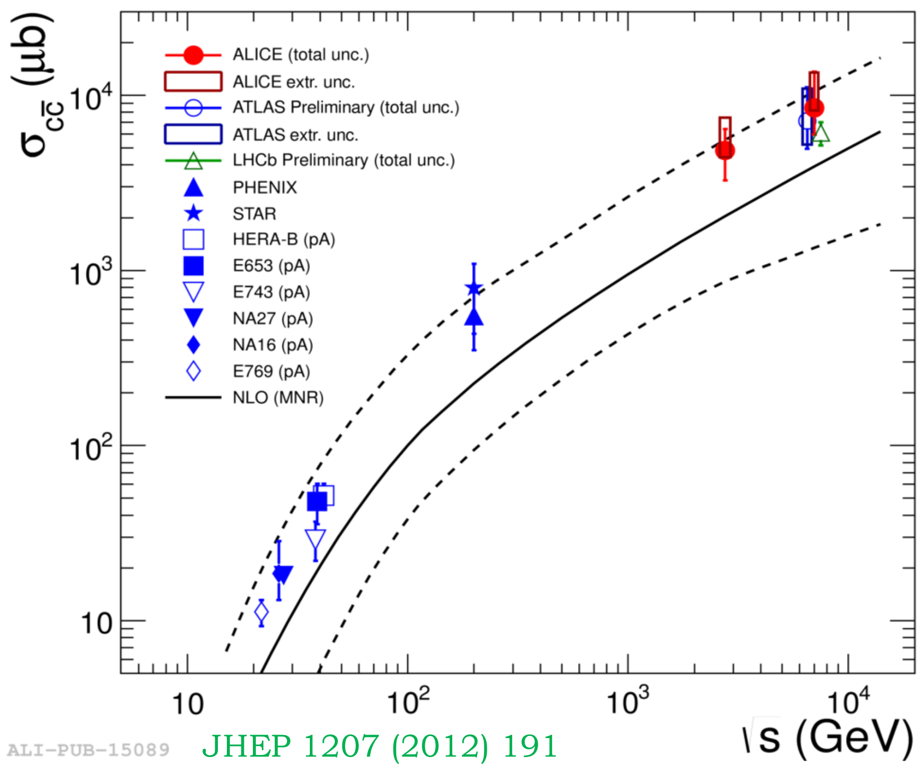

JHEP 1207 (2012) 191

All data points lie in the upper band of the NLO MNR predictions.

$e, \mu \leftarrow$ HF in pp

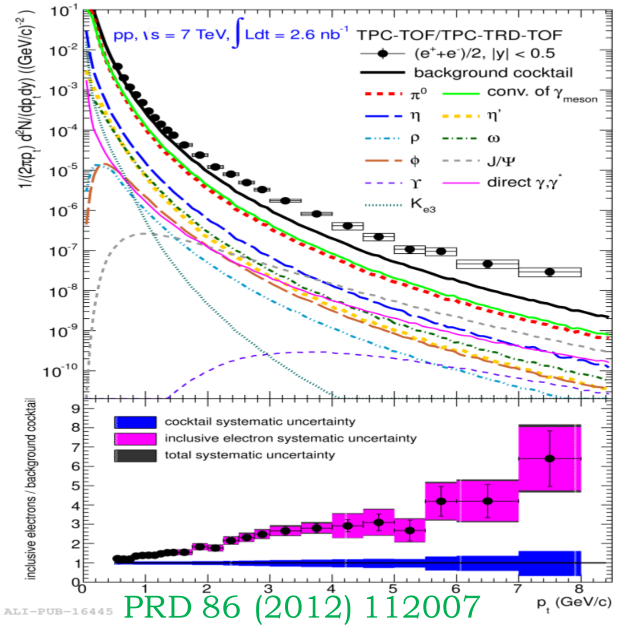

PRD 86 (2012) 112007

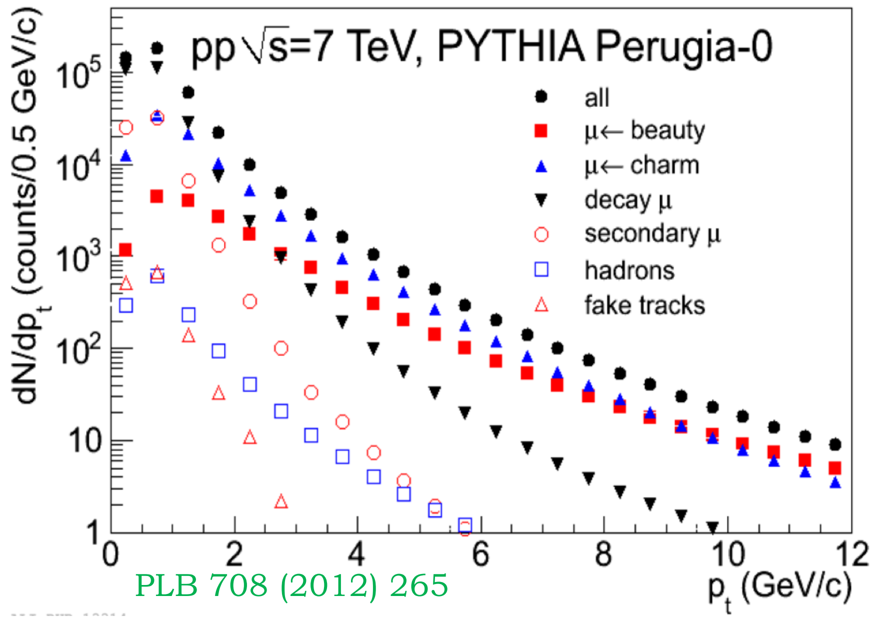

PLB 708 (2012) 265

Measured the inclusive spectrum of $e \leftarrow$ HF and $\mu \leftarrow$ HF.
Background subtracted with simulations: inclusive – background = $l \leftarrow$ HF.

$e, \mu \leftarrow$ HF in pp

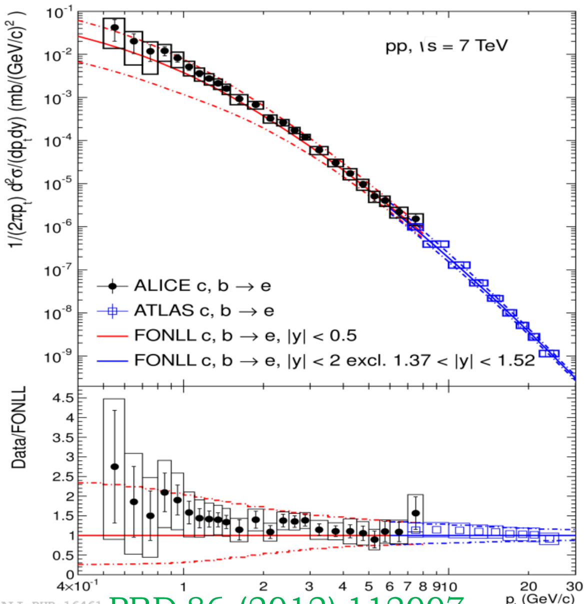

PRD 86 (2012) 112007

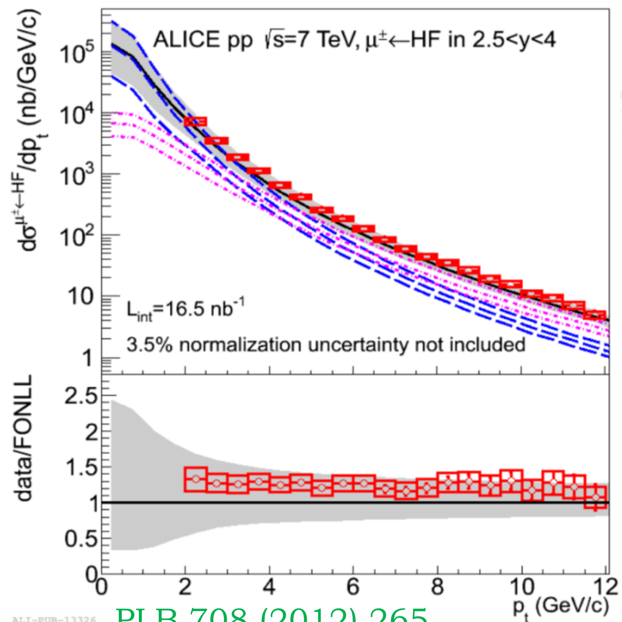

PLB 708 (2012) 265

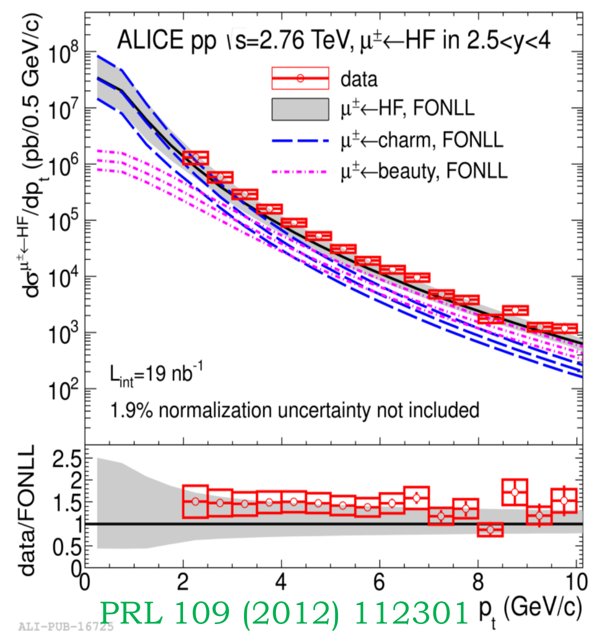

PRL 109 (2012) 112301

Measured the inclusive spectrum of e ← HF and μ ← HF.
Background subtracted with simulations: inclusive – background = $l \leftarrow$ HF.

ALICE complements ATLAS results in the low-p_T regime.
FONLL provides a good description of the results.

e ← HF

Differential cross-sections well described by FONLL.
Beauty contribution is dominant at high-p_T.

μ ← HF

e, μ ← HF in pp

PLB 721 (2013) 13

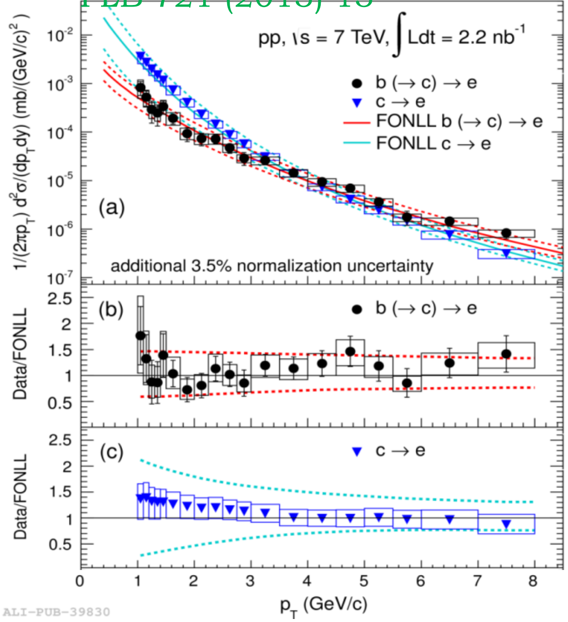

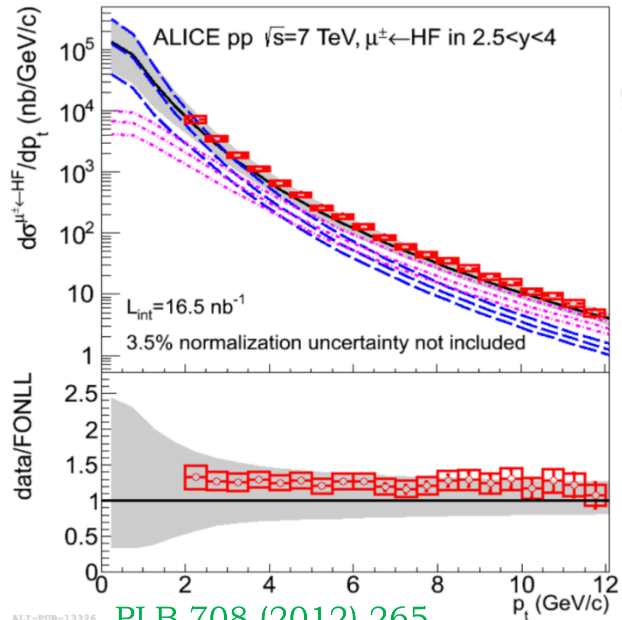

PLB 708 (2012) 265

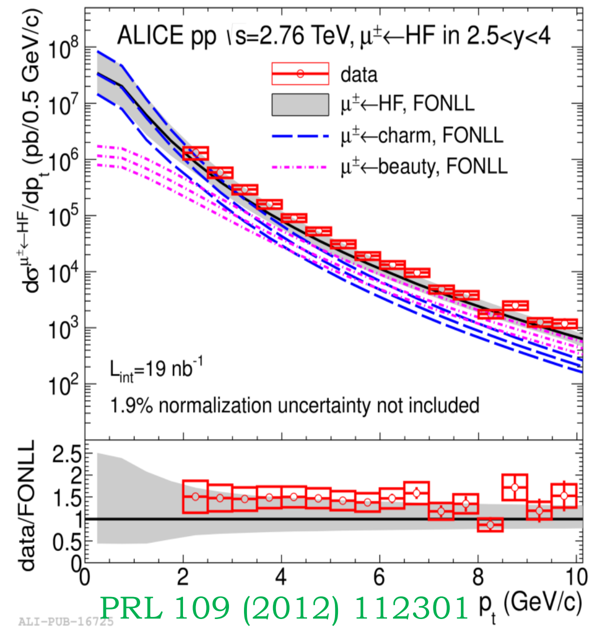

PRL 109 (2012) 112301

Measured the inclusive spectrum of e ← HF and μ ← HF.
Background subtracted with simulations: inclusive – background = l ← HF.

ALICE complements ATLAS results in the low-p_T regime.
FONLL provides a good description of the results.

e ← HF

Differential cross-sections well described by FONLL.
Beauty contribution is dominant at high-p_T.

μ ← HF

D mesons in pPb

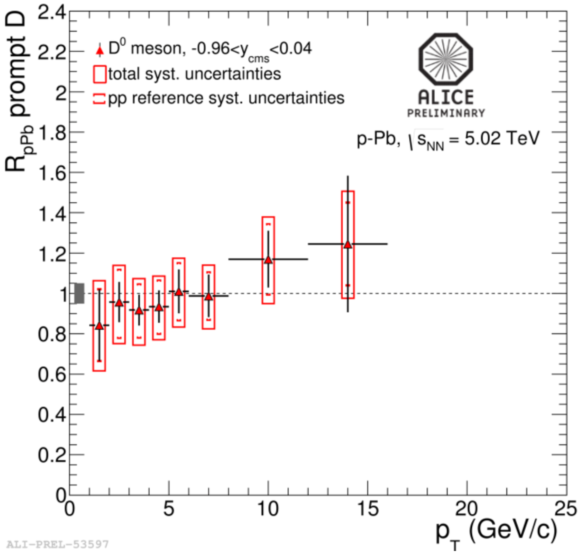

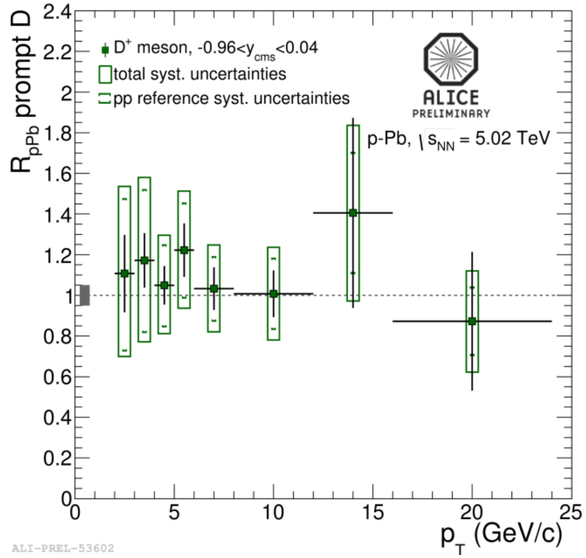

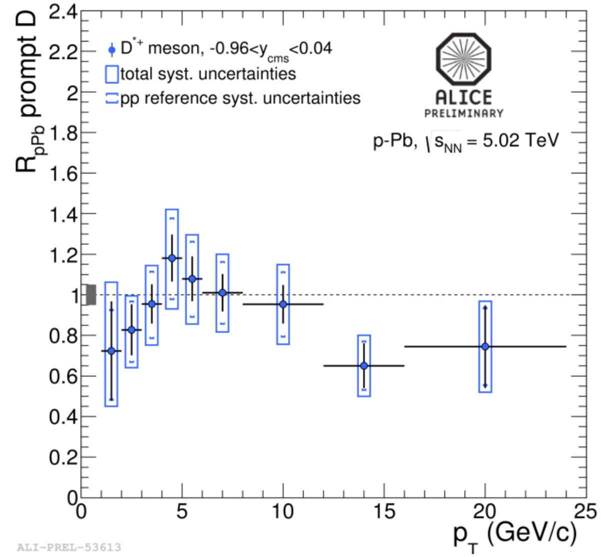

Similar R_{pPb} for D mesons: all measurements compatible (within uncertainties) with unity.

D mesons in pPb

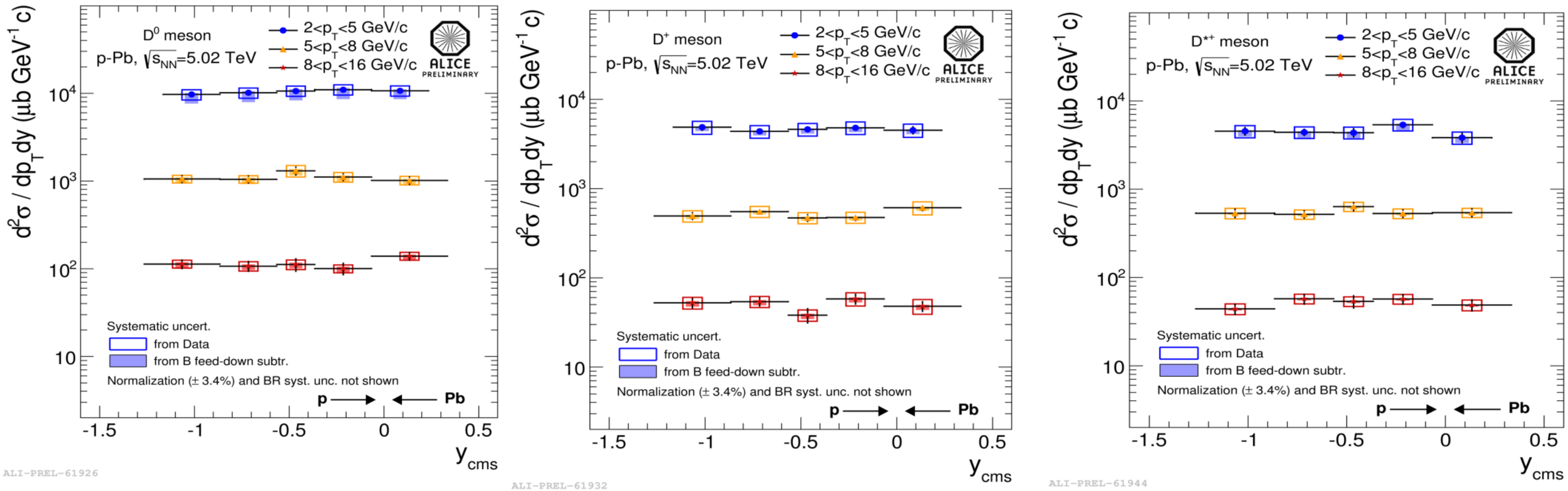

Similar R_{pPb} for D mesons: all measurements compatible (within uncertainties) with unity.

$d^2\sigma/dydp_T$: no rapidity dependence observed in -1.2 < y < 0.3 for all D mesons in three different p_T bins.

D mesons in pPb

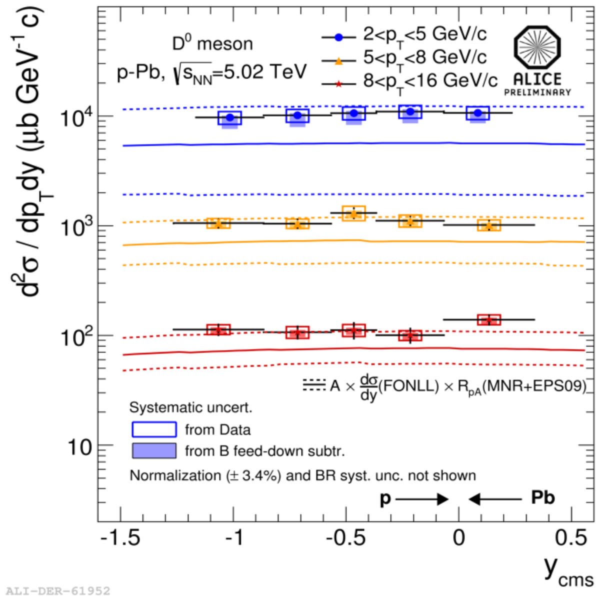

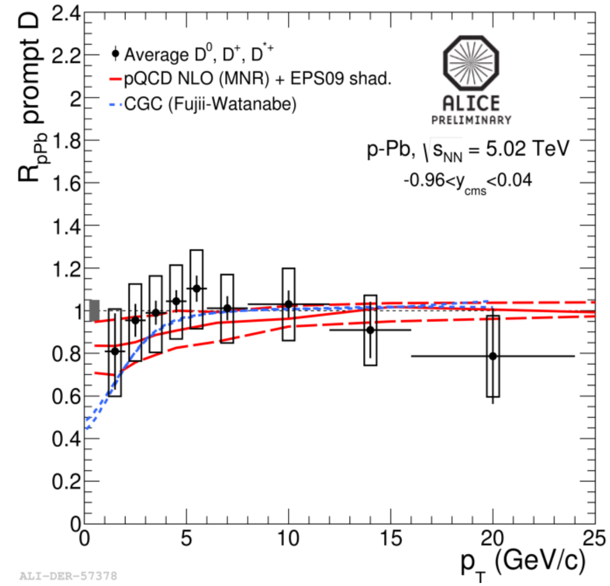

Similar R_{pPb} for D mesons: all measurements compatible (within uncertainties) with unity.

$d^2\sigma/dydp_T$: no rapidity dependence observed in $-1.2 < y < 0.3$ for all D mesons in three different p_T bins.

Transverse momentum and rapidity trends in agreement with pQCD + EPS09 shadowing calculations. CGC model also reproduces the p_T dependence.

$e \leftarrow$ HF in pPb

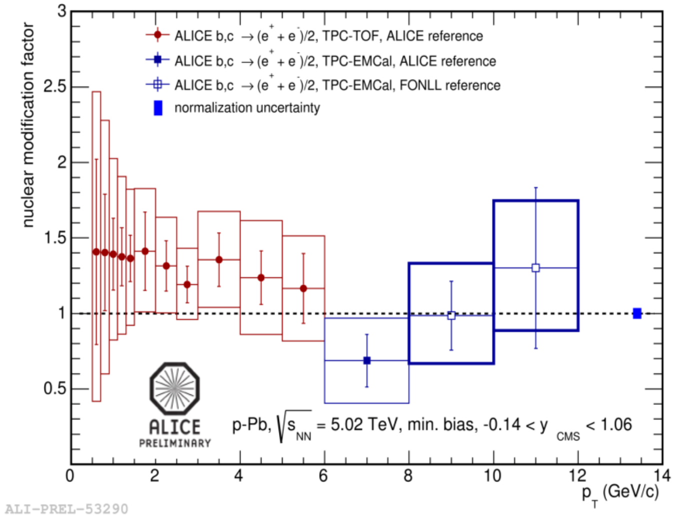

Analysis performed with two different PID techniques depending on the p_T.

$e \leftarrow$ HF in pPb

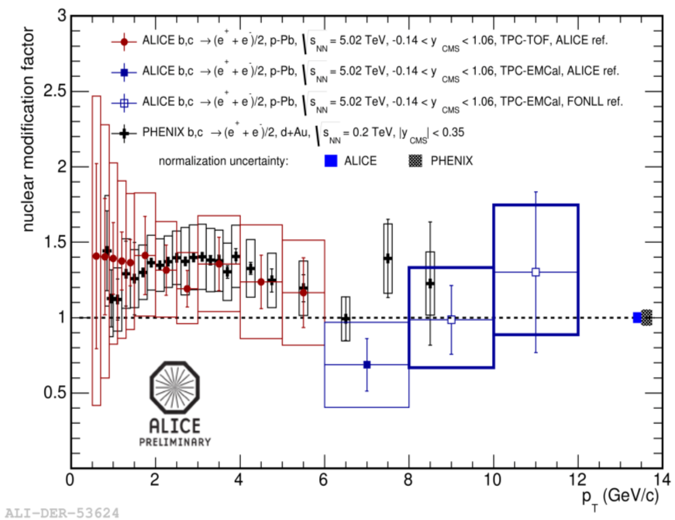

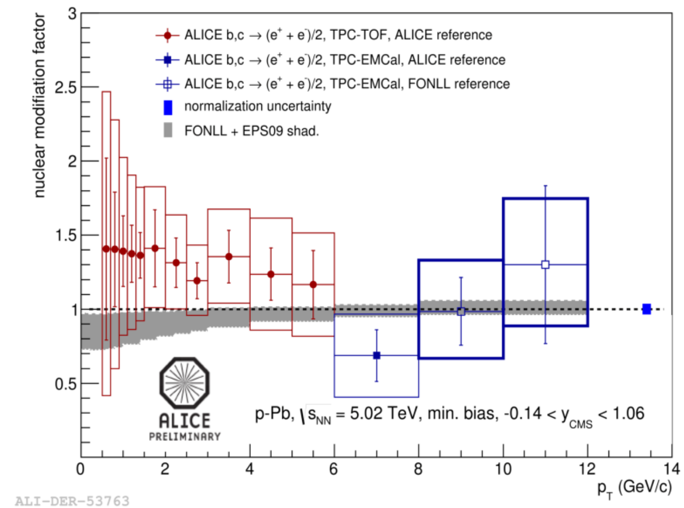

Analysis performed with two different PID techniques depending on the p_T.

R_{pPb} is compatible with unity. Similar results obtained by the PHENIX experiment at lower energy (200 GeV).

FONLL calculation for heavy flavour production with EPS09 shadowing parametrisation can reproduce the data.

D mesons in Pb-Pb

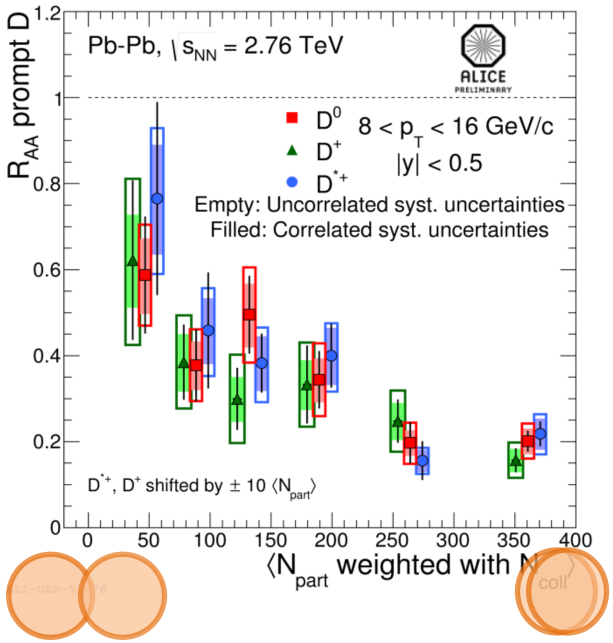

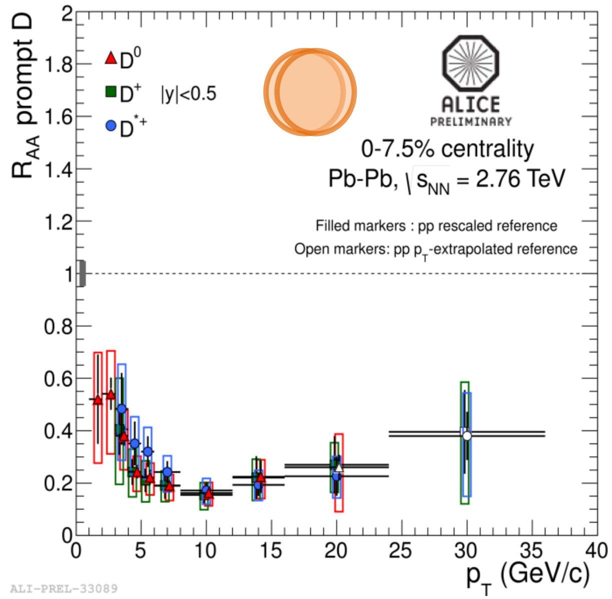

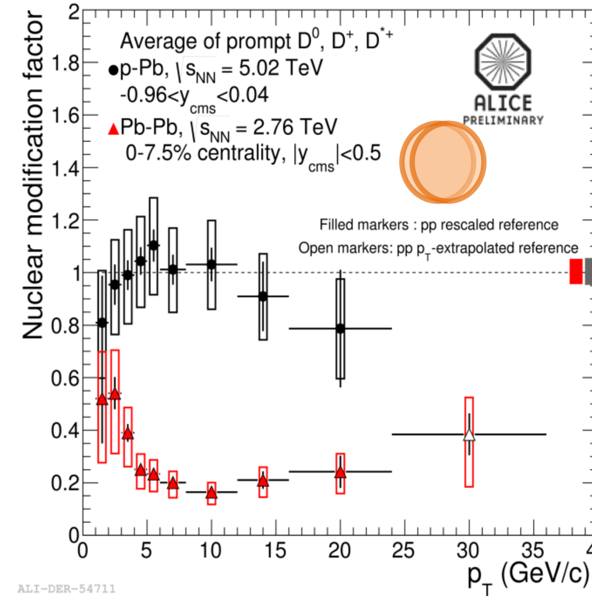

R_{AA} vs centrality: similar suppression for D mesons with and important centrality dependence.

R_{AA} vs p_T: same dependence for all D mesons. Strong suppression at 10 GeV/c (factor 5).

R_{AA} vs R_{pPb}: suppression observed in Pb-Pb collisions due to final state effects!

D mesons in Pb-Pb

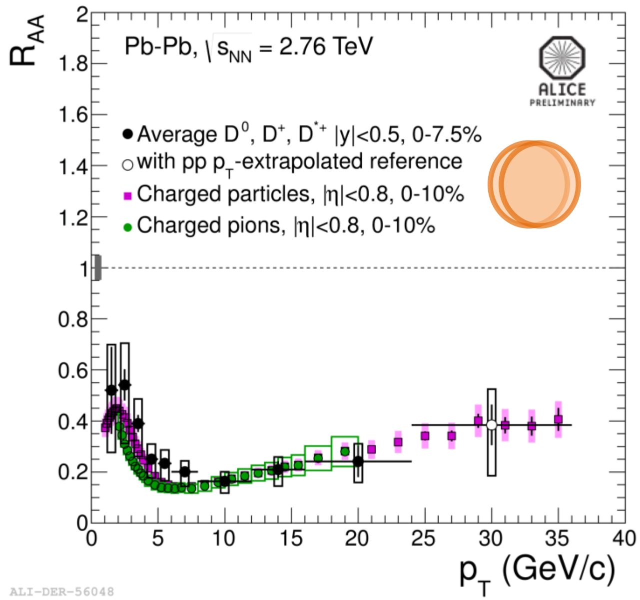

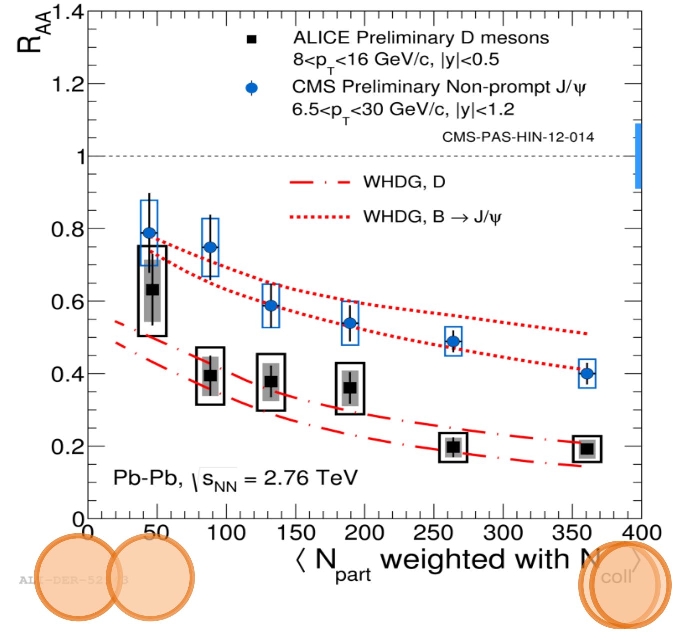

Color charge dependence of energy loss: ΔE(g) > ΔE(c)? Comparison of R_{AA} for pions and D mesons not trivial (different fragmentation functions). R^{D}_{AA} and R^{π}_{AA} in agreement within uncertainties.

Quark mass dependence of energy loss: ΔE(c) > ΔE(b)? D mesons vs non-prompt J/ψ: indication of a larger suppression for charm than for beauty. Well reproduced by models including collisional and radiative energy loss.

$e \leftarrow$ HF in Pb-Pb

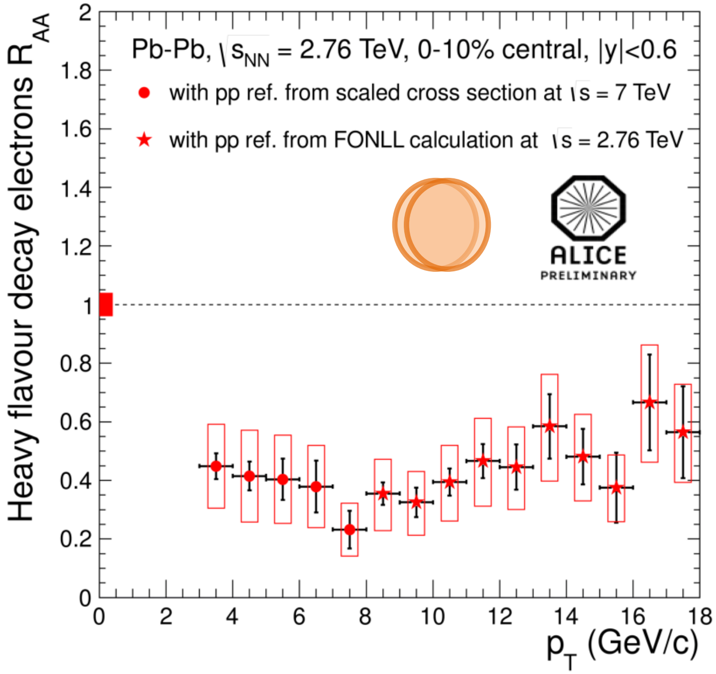

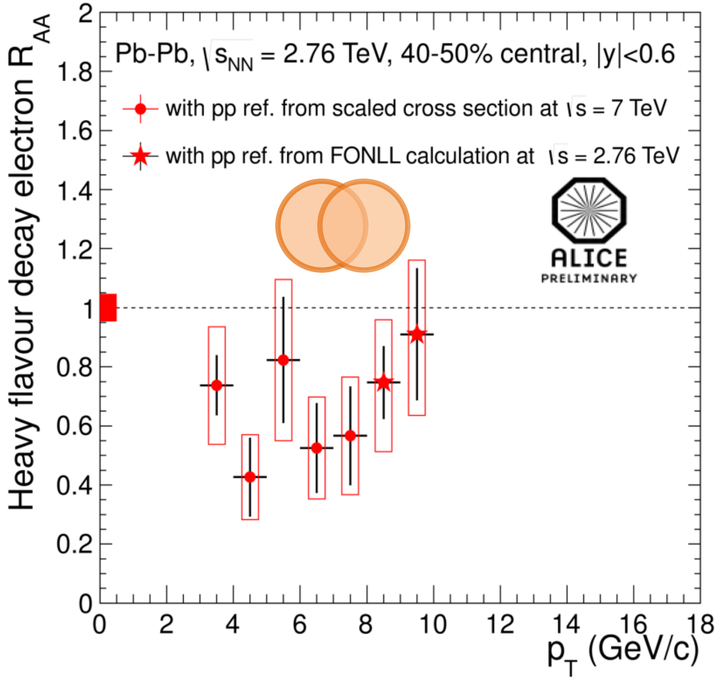

Clear suppression observed for $3 < p_T < 18$ GeV/c for central collisions.

Hint for difference of the HF decay electron R_{AA} measured in central and semiperipheral collisions.

$e, \mu \leftarrow$ HF in Pb-Pb

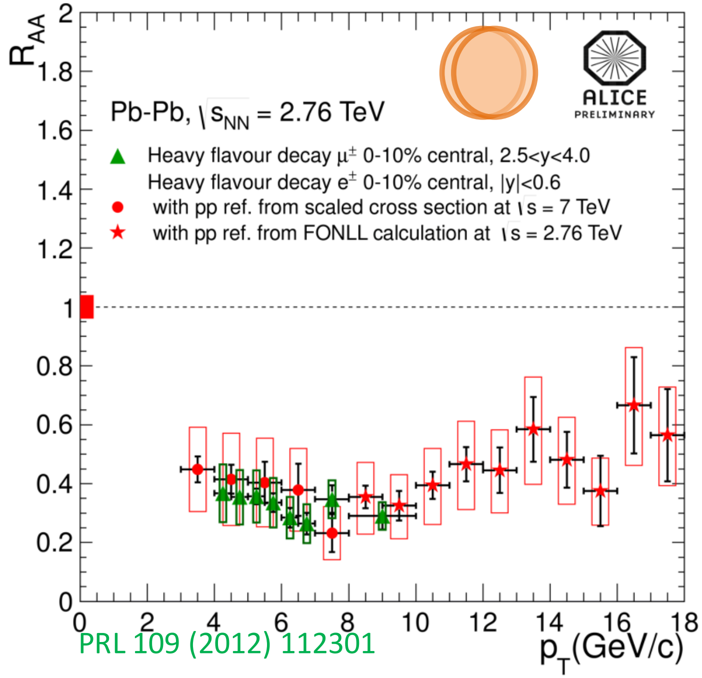

PRL 109 (2012) 112301

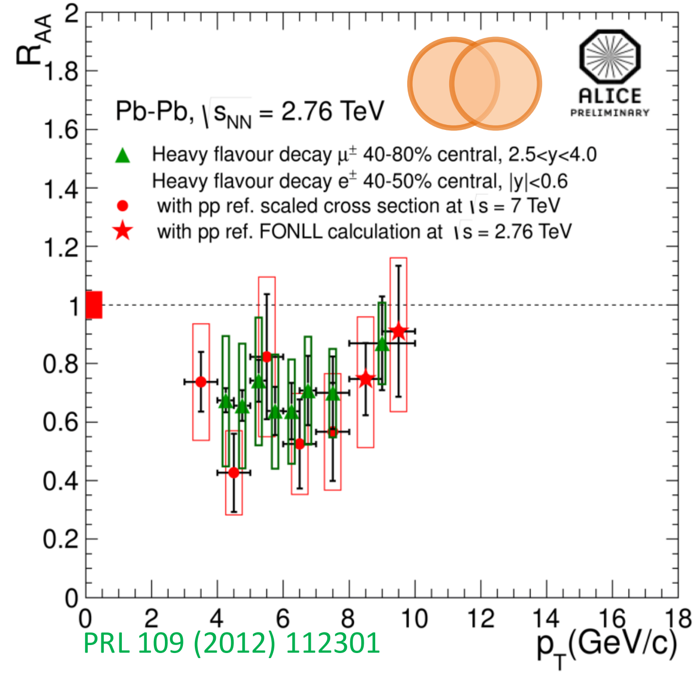

PRL 109 (2012) 112301

Clear suppression observed for 3 (4) < p_T < 18 (10) GeV/c for central collisions.

Hint for difference of the HF decay electron R_{AA} measured in central and semiperipheral collisions.

Similar suppression in mid (electrons) and forward (muons) rapidity.

$\mu \leftarrow$ HF in Pb-Pb

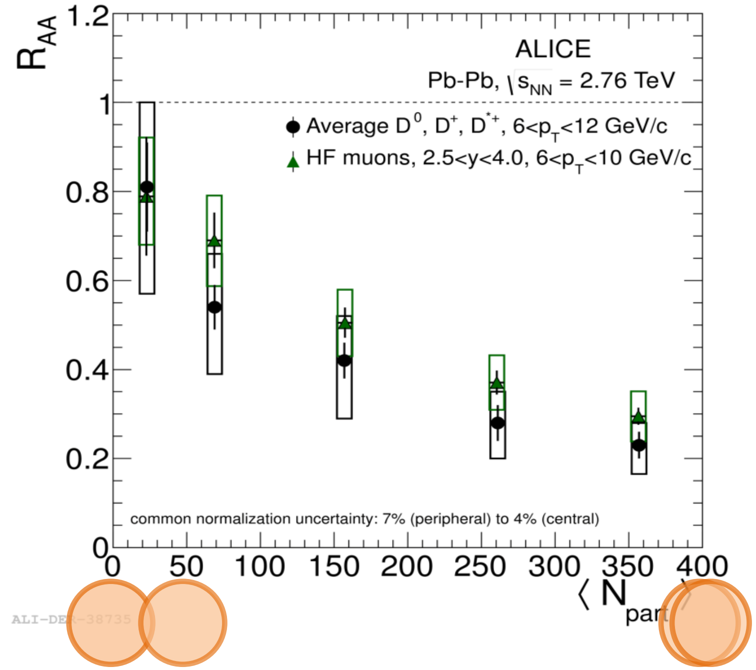

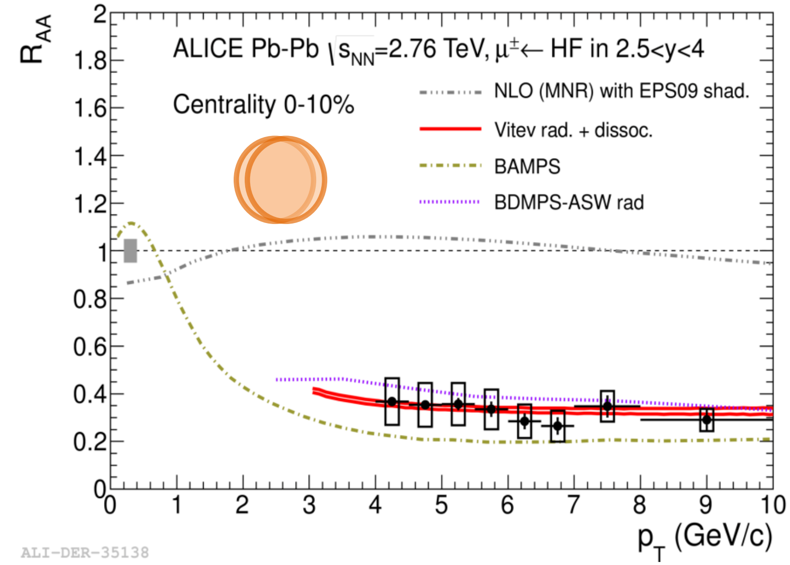

Good agreement between R_{AA} from D mesons (mid rapidity) and R_{AA} from μ←HF (forward rapidity).

μ←HF R_{AA}: well described by models including only radiative energy loss but also radiative plus dissociation energy loss.

Elliptic flow (v_2)

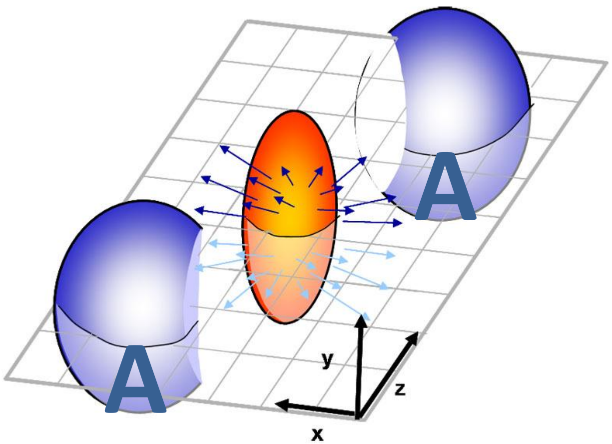

Non central A-A collisions: almond shaped overlap zone determines a preferential direction in the particle emission.

By measuring this anisotropy it is possible to retrieve information of the initial QGP state!

The observable we use is called elliptic flow (v_2).

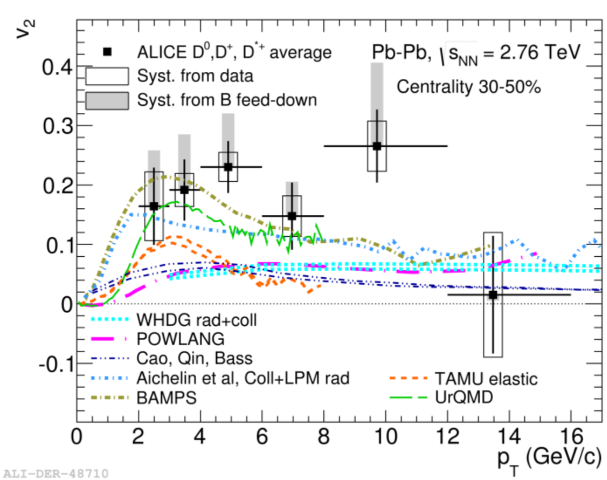

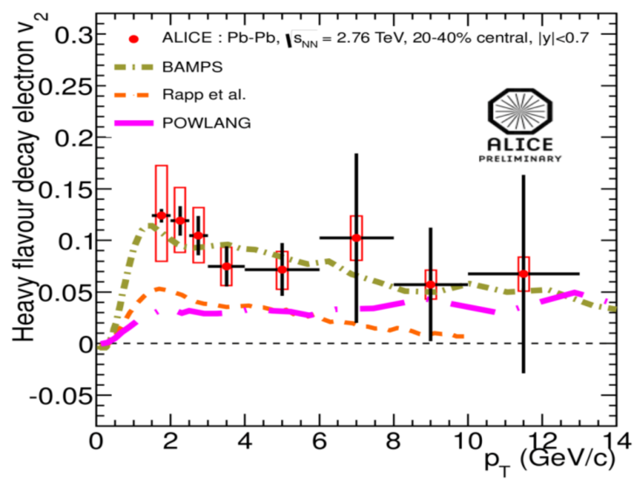

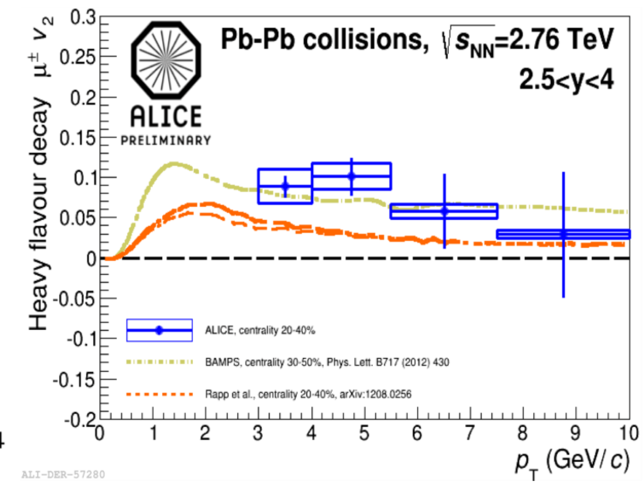

$v_2 > 0$ at low p_T indicates that heavy flavours inherit the azimutal anisotropy produced by the collective expansion of the fireball.

QUARKONIA

ALICE performance

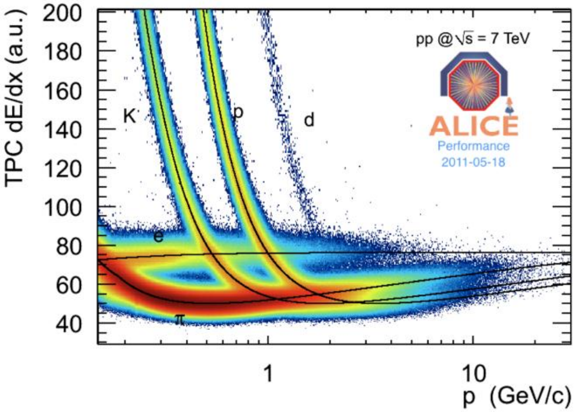

ALICE is unique at the LHC

J/ψ measurements, both at mid and forward rapidity, are performed down to $p_T = 0$ GeV/c.

Electron identification via the specific energy loss (dE/dx) in the TPC.

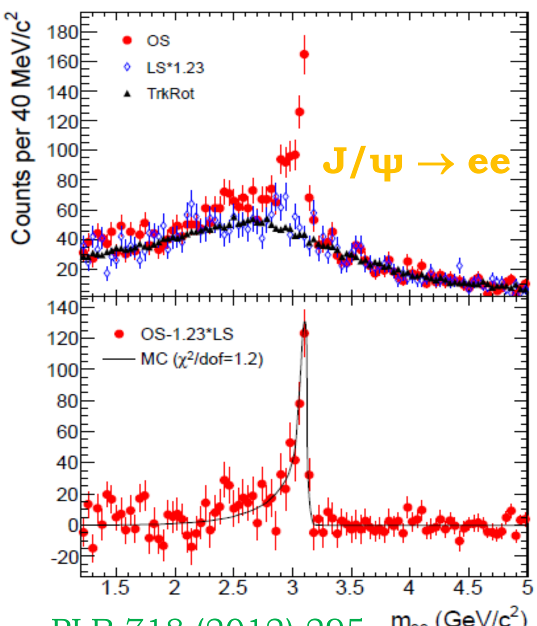

PLB 718 (2012) 295

Muons are identified by requiring that they fire the muon trigger system.

Very good performance in J/ψ detection in a large rapidity range!

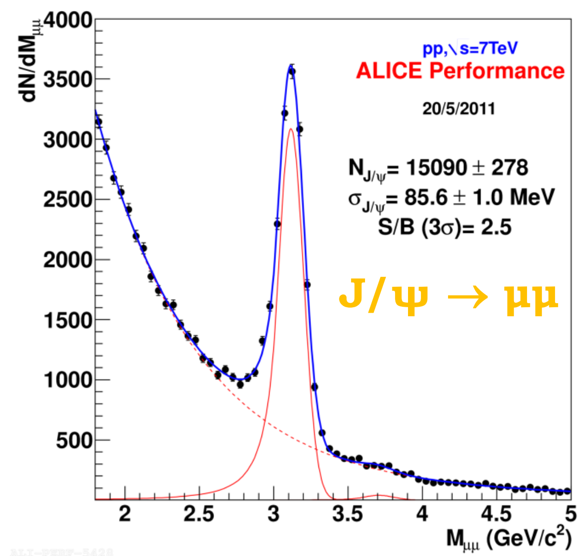

Inclusive J/ψ cross-sections in pp

Mid rapidity: ALICE complements ATLAS and CMS results. Forward rapidity: good agreement with LHCb measurements.

$2.5 < y < 4.0$: NRQCD calculations describe the measured $d^2\sigma/dydp_T$ at 7 and 2.76 TeV.

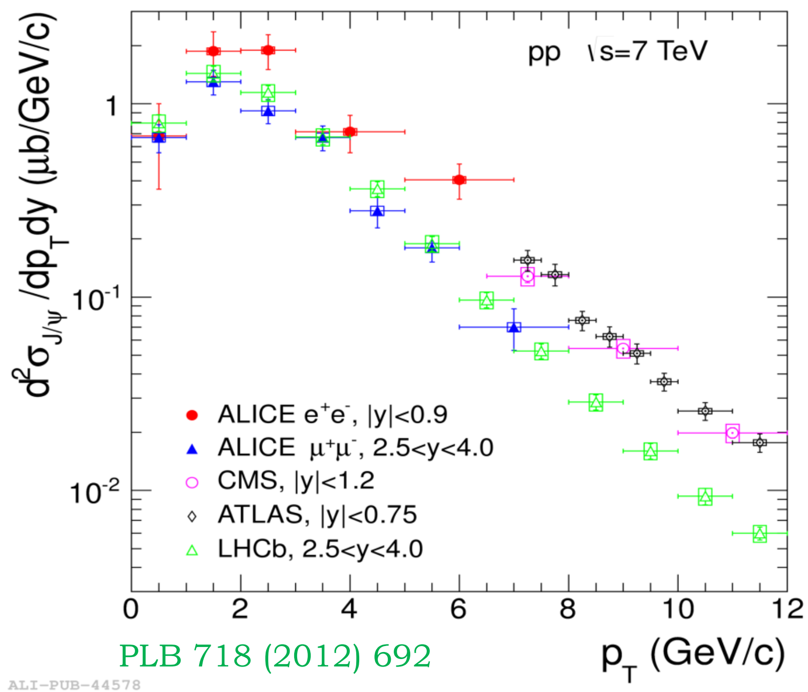

PLB 718 (2012) 692

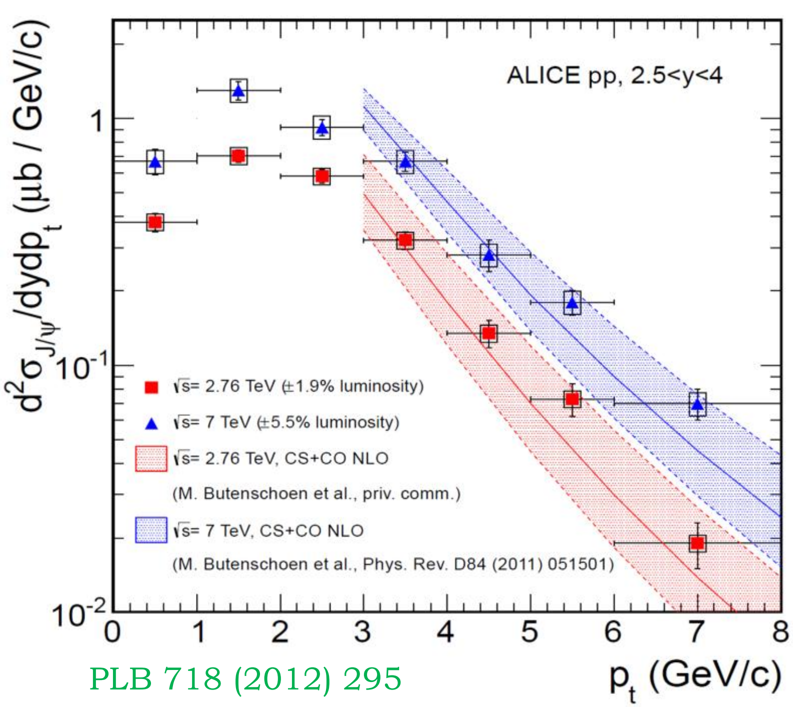

PLB 718 (2012) 295

J/ψ polarization & yield vs multiplicity in pp

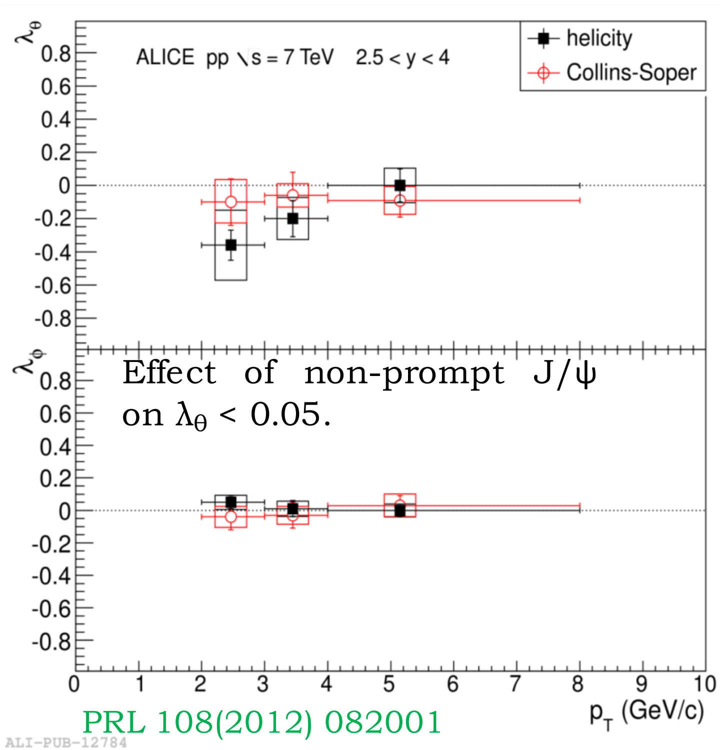

PRL 108(2012) 082001

No significant polarization observed for p_T < 8 GeV/c.

Hint of longitudinal polarization at low-p_T in the helicity frame.

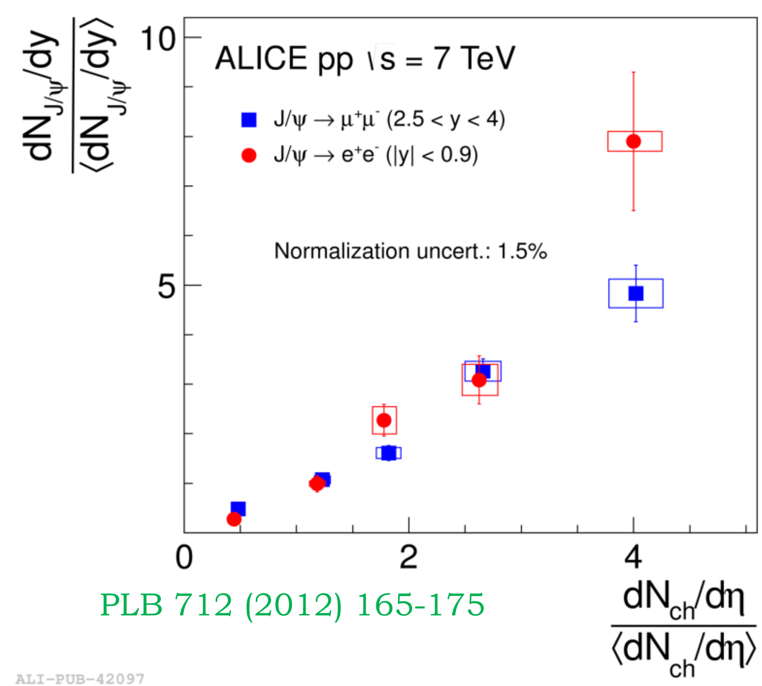

PLB 712 (2012) 165-175

Relative J/ψ production yield vs relative charged particle multiplicity density: observed an approximately linear increase in both rapidity regions.

J/ψ production accompanied by a strong hadronic activity (MPI).

J/ψ polarization & yield vs multiplicity in pp

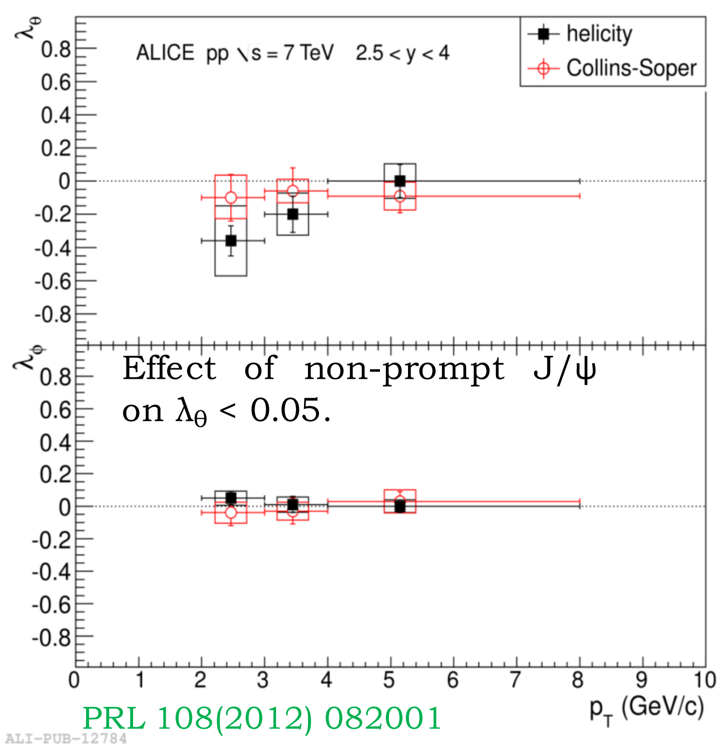

PRL 108(2012) 082001

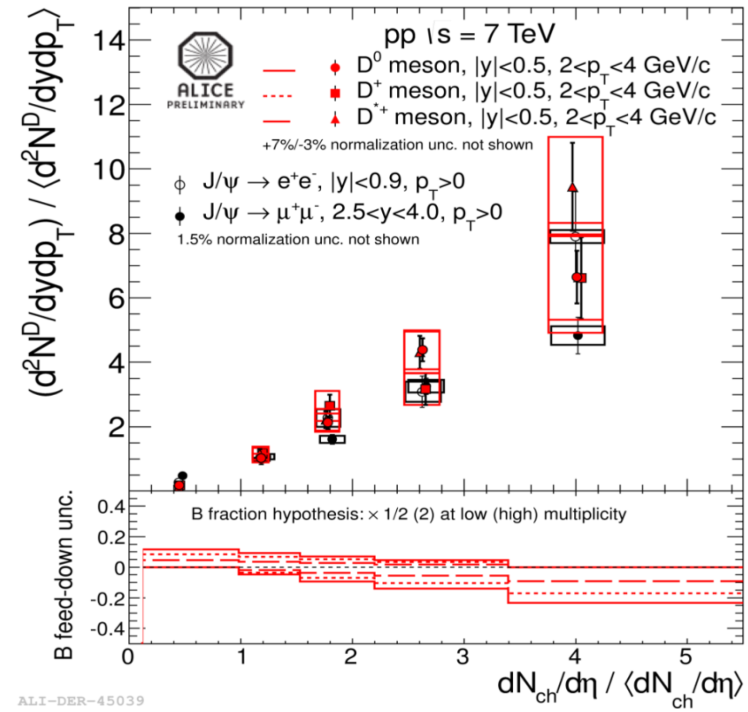

No significant polarization observed for p_T < 8 GeV/c.

Hint of longitudinal polarization at low-p_T in the helicity frame.

Relative J/ψ/D production yield vs relative charged particle multiplicity density: observed an approximately linear increase in both rapidity regions.

J/ψ/D production accompanied by a strong hadronic activity (MPI).

Prompt/non-prompt J/ψ in pp

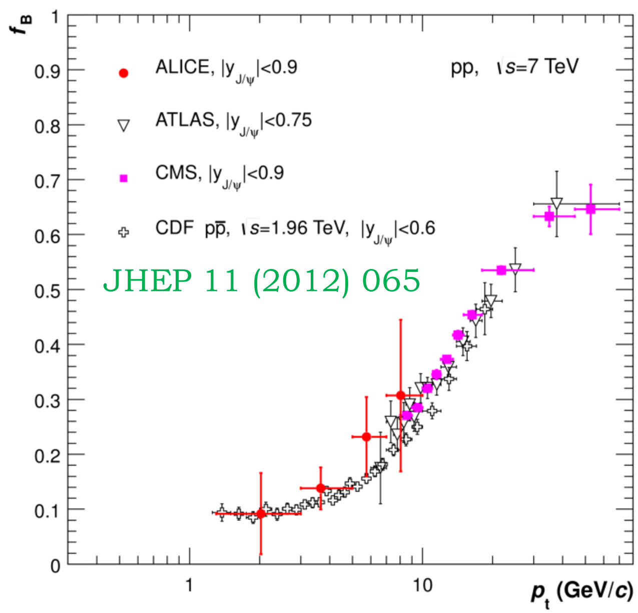

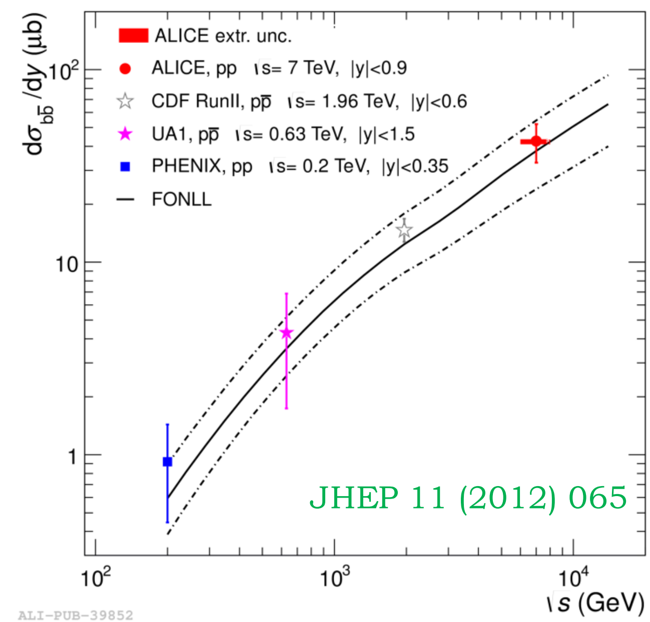

Contribution of non-prompt J/ψ measured by ALICE ranges from 10% (at low- p_T) up to 30% ($p_T \approx$ 10 GeV/c).

ALICE complements ATLAS and CMS measurments by extending the p_T reach down to ≈ 1 GeV/c.

B production cross-section at mid rapidity from ALICE and lower energy experiments are well described by FONLL calculations.

J/ψ in pPb

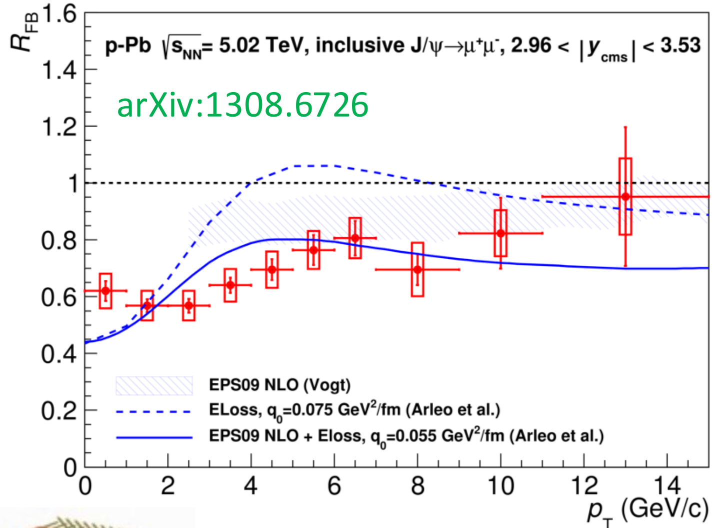

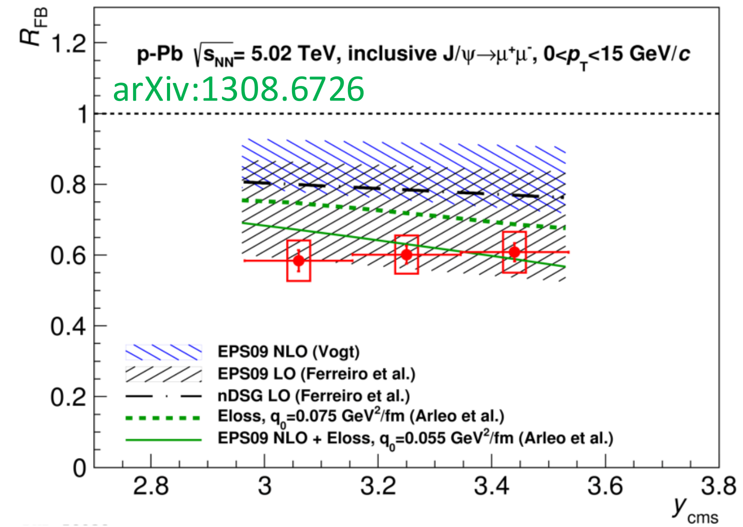

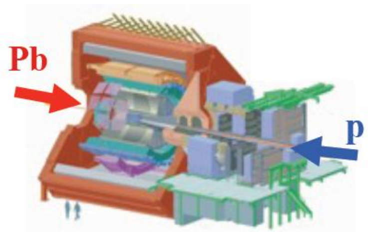

$-4.46 < y_{CMS} < -2.96$

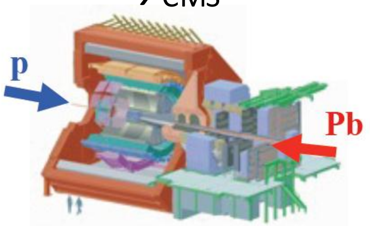

$2.03 < y_{CMS} < 3.53$

$R_{FB}(|y_{CMS}|)=R_{pPb}(|y_{CMS}|)/R_{Pbp}(|y_{CMS}|)$, in the overlapping $|y_{CMS}|$ region.

R_{FB} vs p_T: pure shadowing model tends to overestimate the data. Better agreement with the model including shadowing and energy loss.

R_{FB} vs y: no rapidity dependence. Shadowing + energy loss model has a good description of the results.

J/ψ, ψ(2S) and ϒ(1S) in pPb

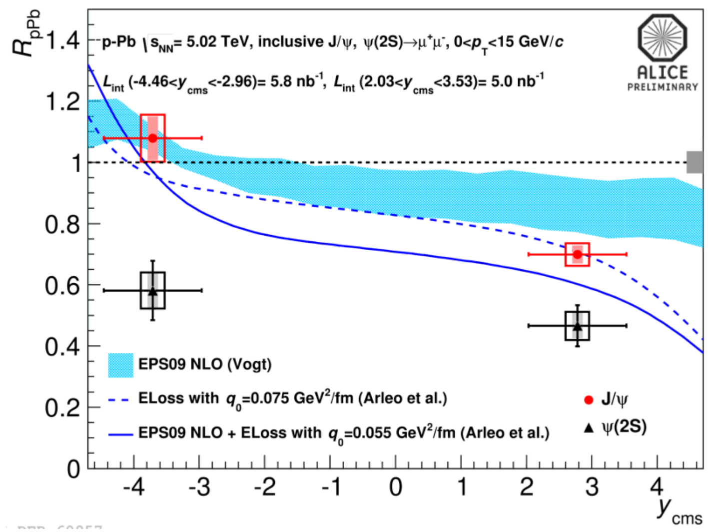

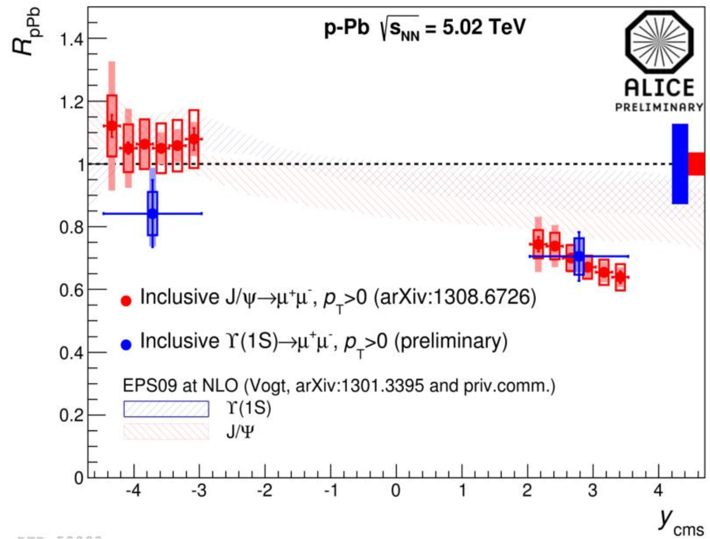

J/ψ: pure shadowing reproduces backward component. At forward rapidity a strong shadowing scenario is favoured.

ψ(2S): stronger suppression relative to J/ψ not described by models ➔ final state effect? Other mechanism?

ϒ(1S): seems to be more suppressed than the prediction from EPS09 at NLO. However, large error on data prevents a firm conclusion.

J/ψ in Pb-Pb

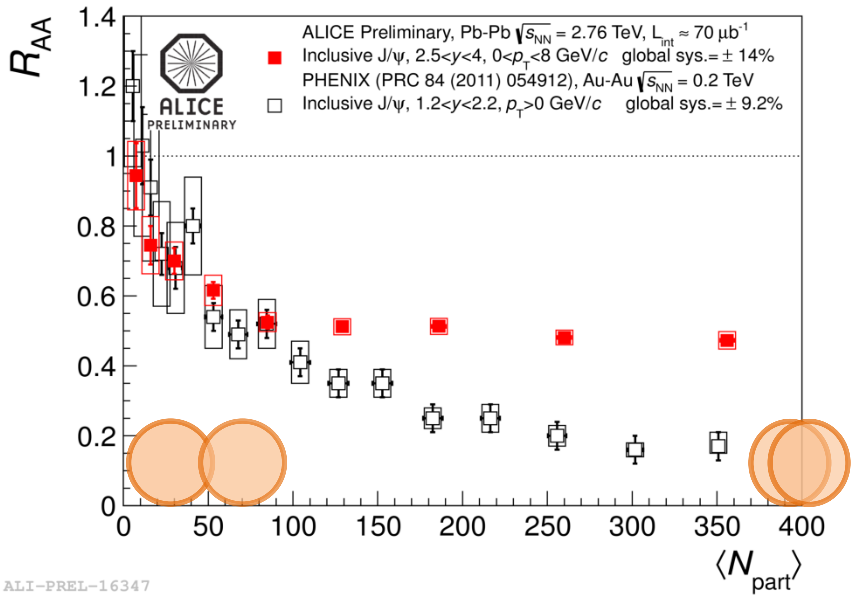

No centrality dependence for N_{part} > 70.

$R_{AA}^{ALICE} \sim 3 \times R_{AA}^{PHENIX}$ for the most central collisions.

J/ψ in Pb-Pb

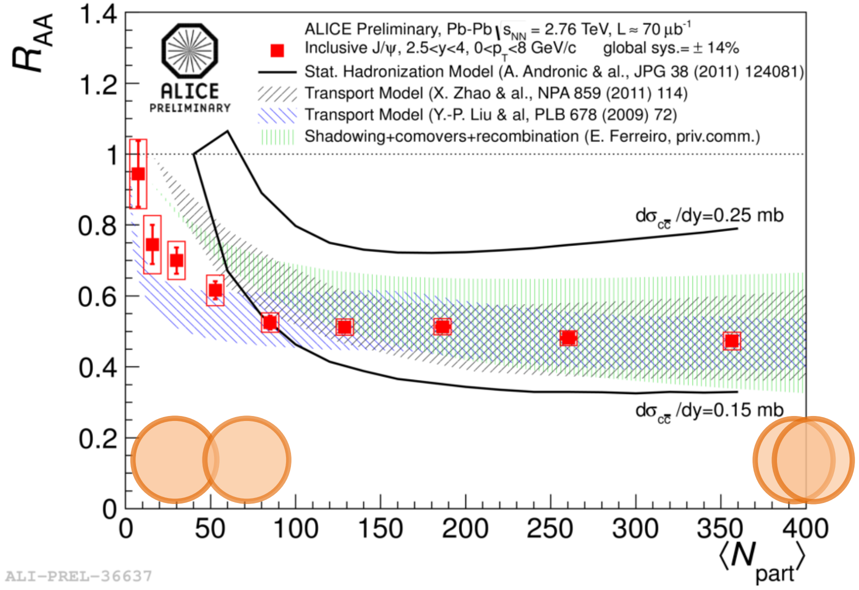

No centrality dependence for $N_{\text{part}} > 70$.

$R_{\text{AA}}^{\text{ALICE}} \sim 3 \text{ x } R_{\text{AA}}^{\text{PHENIX}}$ for the most central collisions.

Data well reproduced by models containing a (re)generation component.

J/ψ in Pb-Pb

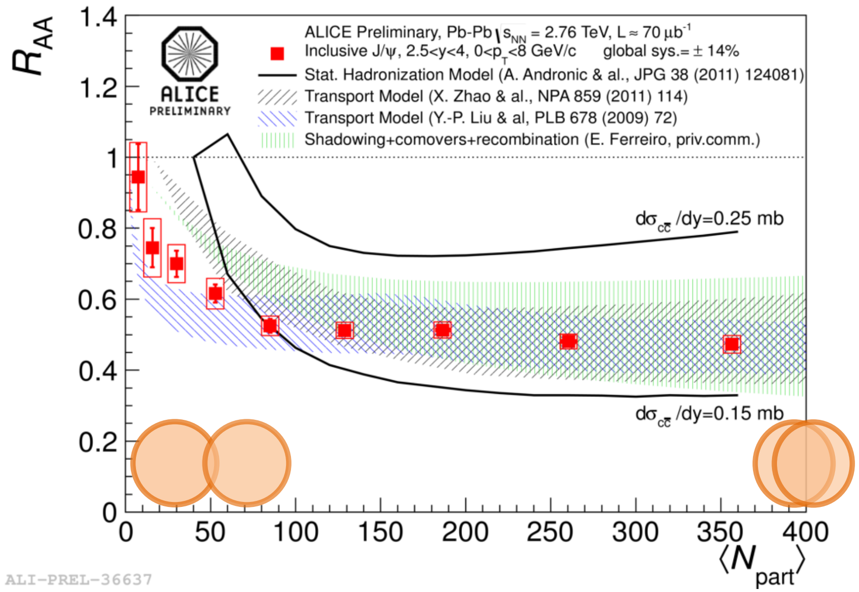

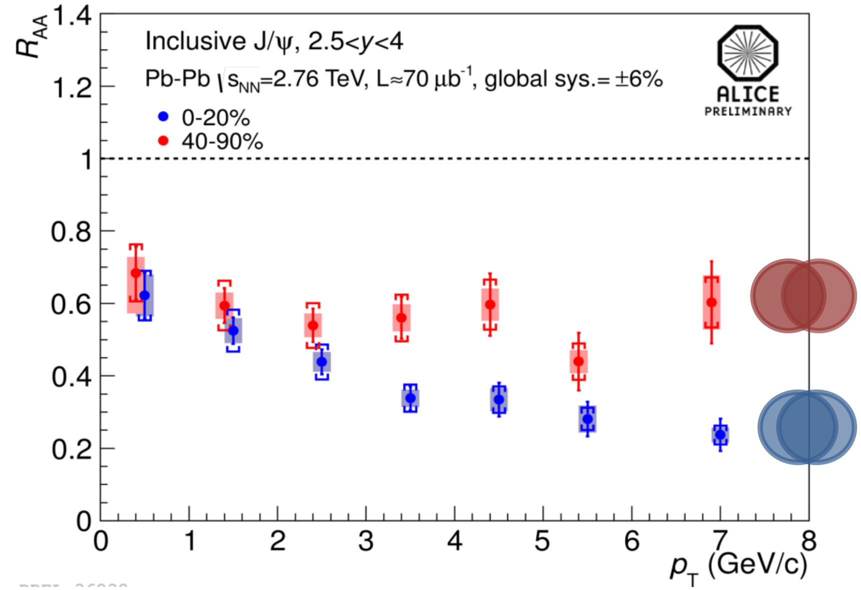

No centrality dependence for $N_{\mathrm{part}} > 70$.

$R_{\mathrm{AA}}^{\mathrm{ALICE}} \sim 3 \text{ x } R_{\mathrm{AA}}^{\mathrm{PHENIX}}$ for the most central collisions.

Data well reproduced by models containing a (re)generation component.

Stronger p_{T} dependence for central collisions (0-20%).

J/ψ in Pb-Pb

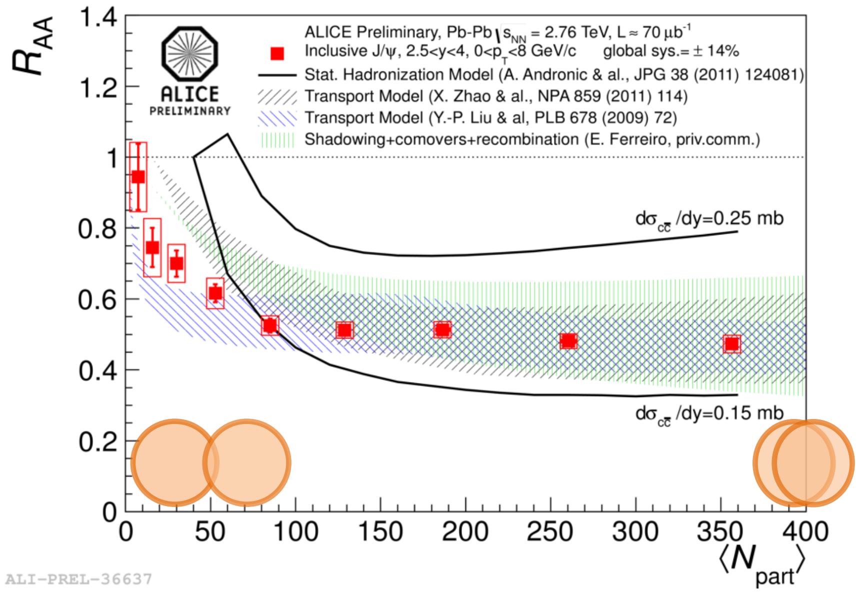

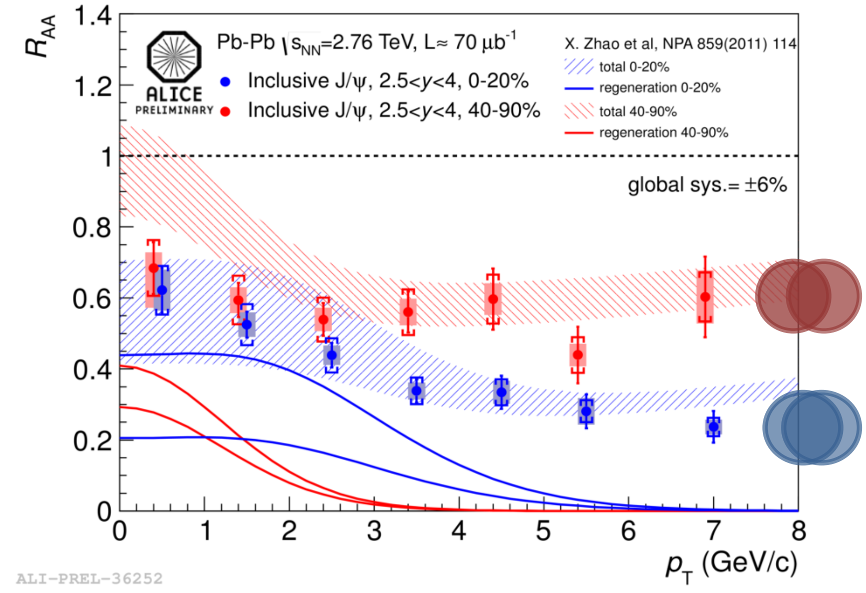

No centrality dependence for $N_{\text{part}} > 70$.

$R_{\text{AA}}^{\text{ALICE}} \sim 3 \text{ x } R_{\text{AA}}^{\text{PHENIX}}$ for the most central collisions.

Data well reproduced by models containing a (re)generation component.

Stronger p_{T} dependence for central collisions (0-20%).

According to the models: regeneration at work in the low-p_{T} regime!

J/ψ and Υ(1S) in Pb-Pb

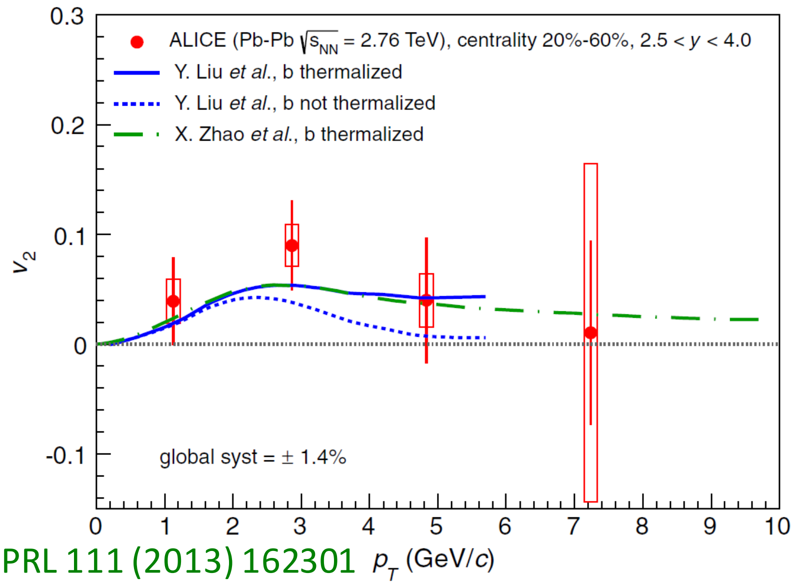

PRL 111 (2013) 162301

J/ψ $v_2 \neq 0$ at 3 GeV/c (2.7 σ) and well reproduced by models including a regeneration component.

J/ψ and ϒ(1S) in Pb-Pb

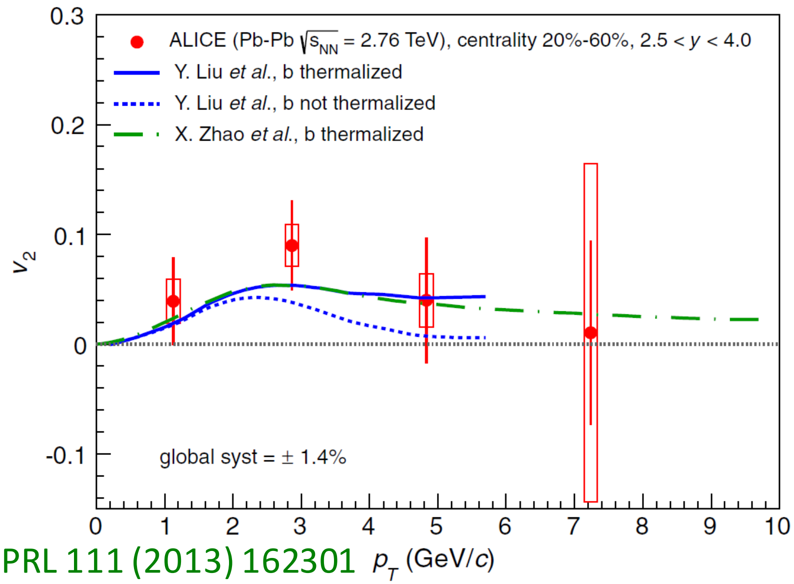

PRL 111 (2013) 162301

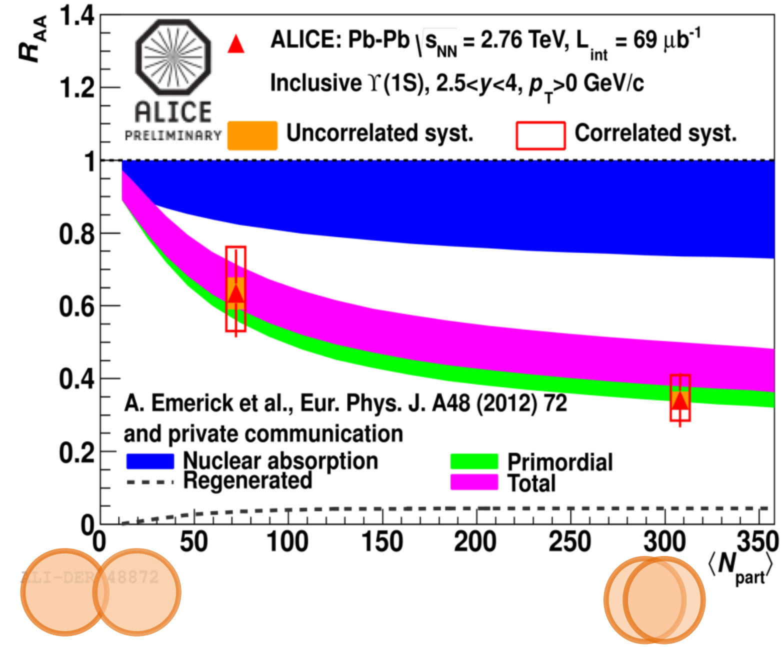

J/ψ $v_2 \neq 0$ at 3 GeV/*c* (2.7 σ) and well reproduced by models including a regeneration component.

Clear ϒ(1S) suppression at forward rapidity.

Model including CNM can reproduce the data. Negligible contribution due to regeneration.

UPGRADES

Motivations

Run I (2009 - 2013): maximum read out in ALICE of 500 Hz.

Run III (> 2018): LHC will reach an interaction rate of 50 kHz with Pb beams.

In this escenario ALICE will focus on low-p_T observables:

- ❑ Not triggerable events (examine full statistics).
- ❑ Detectors will have to become faster.

In this way ALICE will register 10 nb^{-1} of Pb-Pb collisions.

For open heavy flavours and quarkonia this implies:

- ❑ New Inner Tracking System.
- ❑ High-rate upgrade for the Time Projection Chamber and Muon Spectrometer.

\+ A new detector (Muon Foward Tracker) that will extend the scope of ALICE.

Inner Tracking System

CERN-LHCC-2012-013

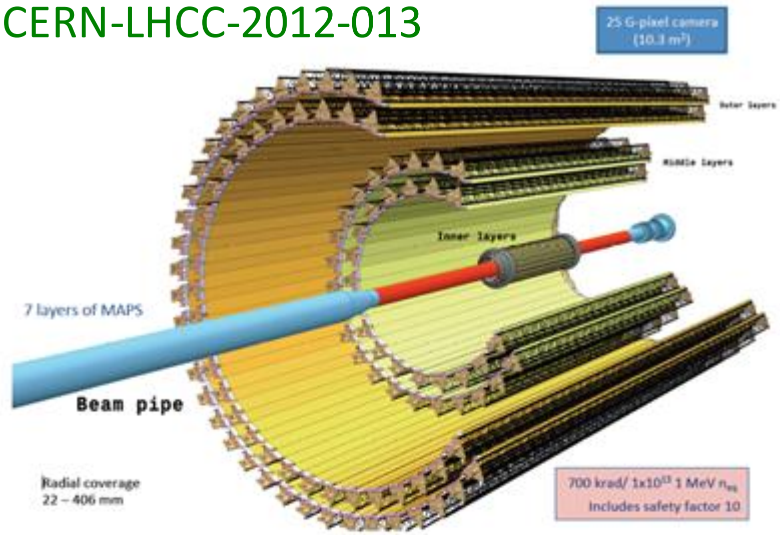

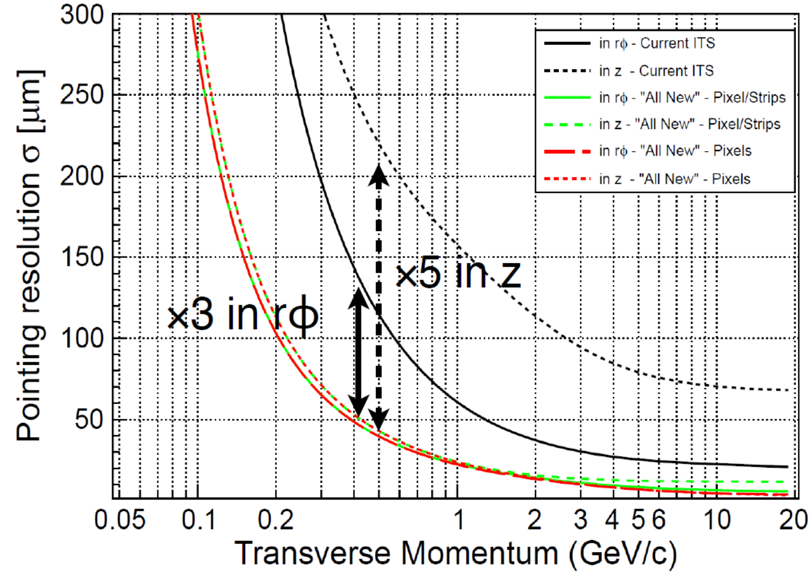

Get closer to IP (first layer): 39 mm to 22 mm.

Increase granularity (6 layers to 7 layers) and reduce pixel size (from 50 x 425 μm to 20 x 20 μm).

Fast readout: pp at 1 MHz and Pb-Pb at 50 kHz.

Improves the pointing resolution by x3 ($r\phi$) and x5 (z).

Reduces the material budget (X/X_0 per layer): from 1.14% to 0.3% for the inner layers.

TPC and Muon Spectrometer

TPC CERN-LHCC-2012-012

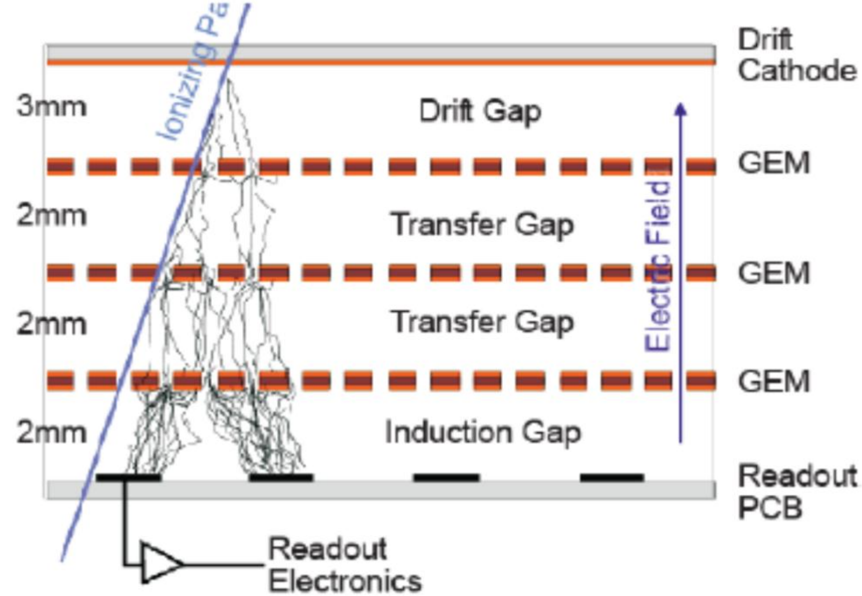

Current performance: 100 μs drift time implies a maximum rate operation of 3.5 kHz.

Move from MWPC to a Gas Electron Multiplier (GEM) detector.

GEM: intrinsic ion blocking and large rate opration.

Muon Spectrometer

Tracking: increase read out rate and keep dead-time below 10%. Trigger: present readout time of 110 μs would imply, during Run III, a dead-time > 30%.

Replace existing front end electronics in order to reduce the read-out time to approximately 20 μs/event.

Muon Forward Tracker

5 (6) silicon pixel discs located in front of the absorber.

MFT will improve the pointing accurancy in the vertex region.

OHF: separate charm and beauty contributions at the (di)muon level.

ψ’: improve the S/B by x6 with respect to the current performance.

J/ψ ← B: prompt/displaced J/ψ separation for measuring B down to zero p_T.

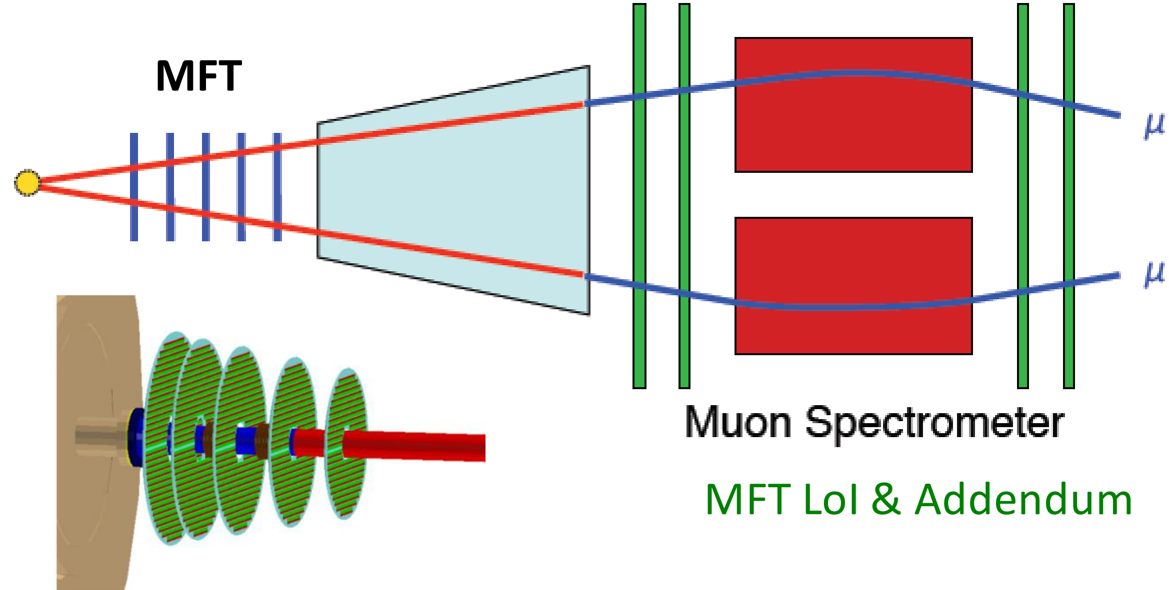

MFT LoI & Addendum

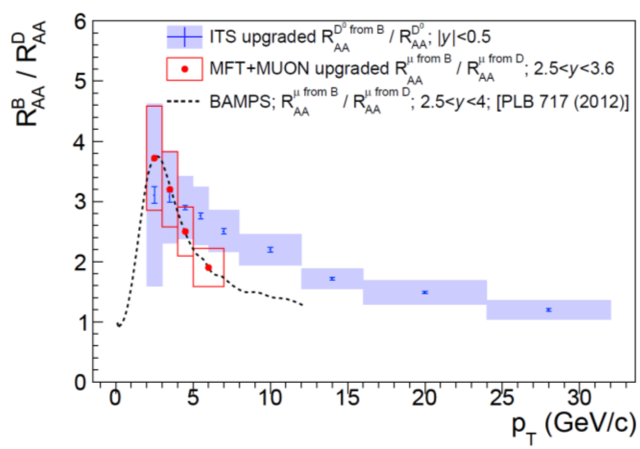

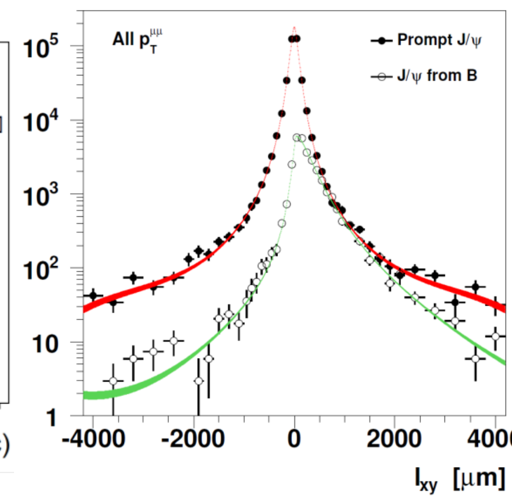

CONCLUSIONS

Conclusions

- In pp collisions:
  - Open HF results are well described by pQCD calculations.
  - J/ψ measurements can be reproduced by NRQCD models.

- In pPb collisions:
  - R_{pPb} compatible with unity for D mesons and e ← HF.
  - Shadowing + energy loss calculation favoured by J/ψ R_{FB}. Strong suppression in ψ(2S) R_{pPb} not reproduced by any model.

- In Pb-Pb collisions:
  - Observed suppression of D mesons is a final state effect.
  - Evidence of J/ψ production from (re)generation at low-p_{T}.

- The upgrades will enhance the physics results on quarkonia and open heavy flavours in ALICE.

Conclusions

- In pp collisions:
  - Open HF results are well described by pQCD calculations.
  - J/ψ measurements can be reproduced by NRQCD models.

- In pPb collisions:
  - R_{pPb} compatible with unity for D mesons and e ← HF.
  - Shadowing + energy loss calculation favoured by J/ψ R_{FB}. Strong suppression in ψ(2S) R_{pPb} not reproduced by any model.

- In Pb-Pb collisions:
  - Observed suppression of D mesons is a final state effect.
  - Evidence of J/ψ production from (re)generation at low-p_T.

- The upgrades will enhance the physics results on quarkonia and open heavy flavours in ALICE.

Je vous remercie de votre attention

BACKUP

ALICE performance

Open heavy flavours in Central Barrel
- Displaced vertex topology.
- Particle Identification.

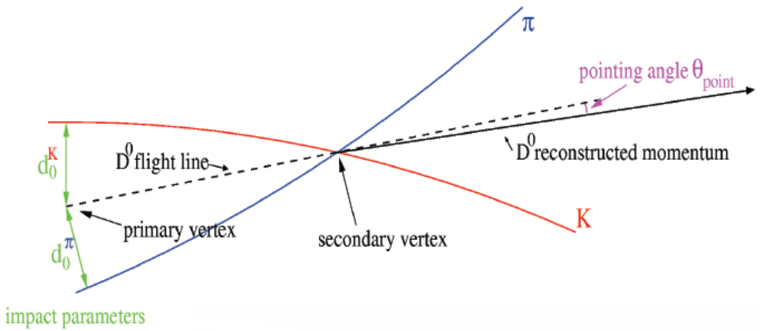

Precise tracking and vertexing needed!
- Primary vertex
- Secondary vertex
- Impact parameter

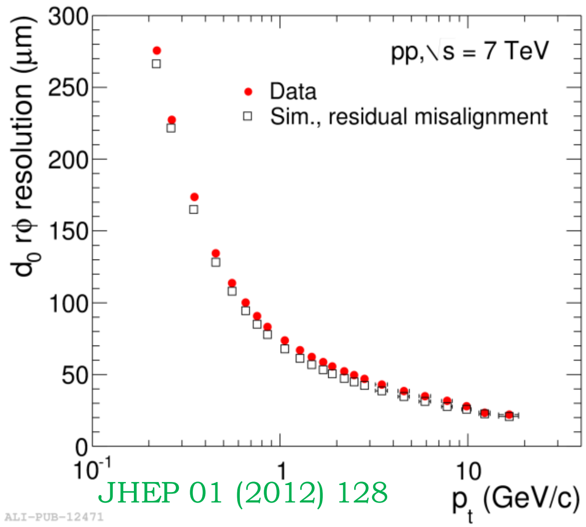

JHEP 01 (2012) 128

ALICE: excellent impact parameter resolution.

PID
- ✓ π/K: TPC and TOF.
- ✓ e: TOF, TPC, TRD and EMCAL.

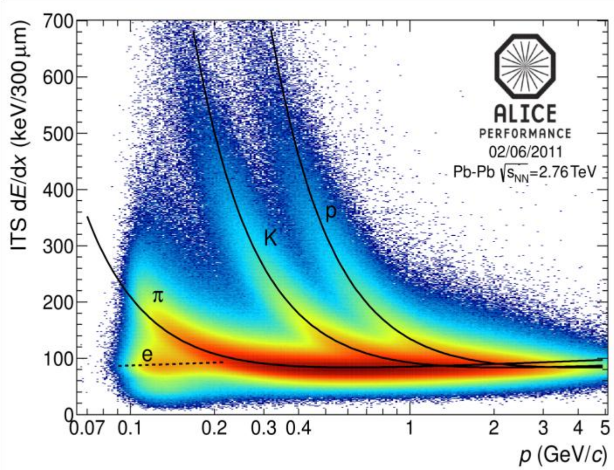

$e \leftarrow B$ @ 7 TeV

Exploit large displacement of B decay electrons ➔ apply impact parameter cut!

Then, subtract remaining background electrons with a cocktail.

Differential cross-sections well described by FONLL.

Low-p_T: e from HF predominantly from charm hadrons.

High-p_T: beauty hadrons become dominant.

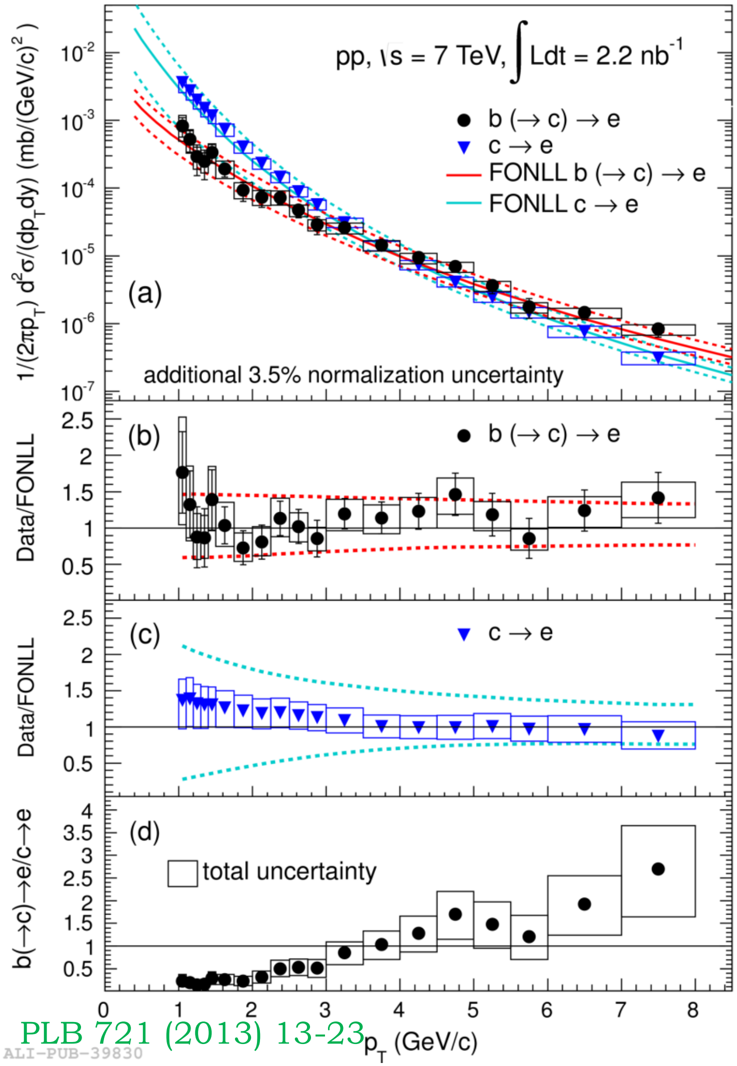

PLB 721 (2013) 13-23

Elliptic flow

The azimuthal momentum distribution is expanded in a Fourier series:

$$\frac{dN}{d\phi} = \frac{N}{2\pi}\left[1 + 2\nu_1 \cos(\phi) + 2\nu_2 \cos(2\phi) + \ldots\right],$$

with ϕ the azimuthal angle of the momentum and ν_n the Fourier coefficients of the n-th harmonic. Due to the symmetry around the *y*-axis the sine terms vanish.

Models

BAMPS: Partonic transport model with collisional and radiative energy loss *PLB 717 (2012) 430*.

Rapp et al. (aka TAMU): Transport model based on collisional processes *arXiv:1208.0256.*

POWLANG: Heavy quark transport approach based on a Langevin equation in an expanding deconfined medium *JPG 38 (2011) 124144*.

Djordjevic et al: radiative energy loss in a finite size dynamical QCD medium *arXiv:1307.4098*.

Vitev et al: radiative energy los plus D mesons in-medium formation and dissociation *PLB 713 (2012) 224.*

Polarization

Inclusive J/ψ polarization measured using the angular distribution of daughter muons in the quarkonium rest frame

$$W(\cos\theta,\phi) \propto \frac{1}{3+\lambda_\theta}(1+\lambda_\theta\cos^2\theta+\lambda_\phi\sin^2\theta\cos 2\phi+\lambda_{\theta\phi}\sin 2\theta\cos\phi)$$

$\lambda_\theta = +1 \rightarrow$ transverse polarization

$\lambda_\theta = 0 \rightarrow$ no polarization

$\lambda_\theta = -1 \rightarrow$ longitudinal polarization

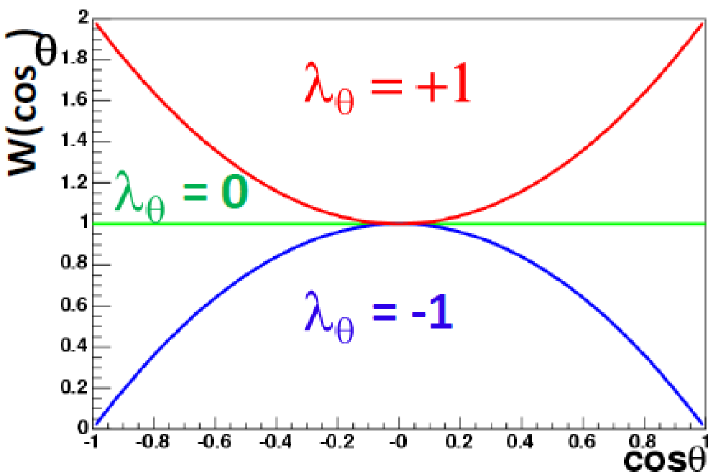

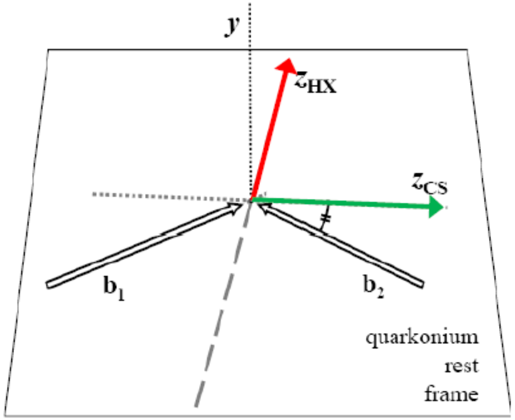

Two different definitions of *z*-axis considered

- Helicity: direction of the decaying particle in the CM frame of the collision.
- Collins-Soper: bisector of the angle between one beam and the opposite of the direction of the other one, in the rest frame of the decaying particle.

Polarization

ALICE results compared to LO and NLO predictions from **NRQCD** and **CSM**.

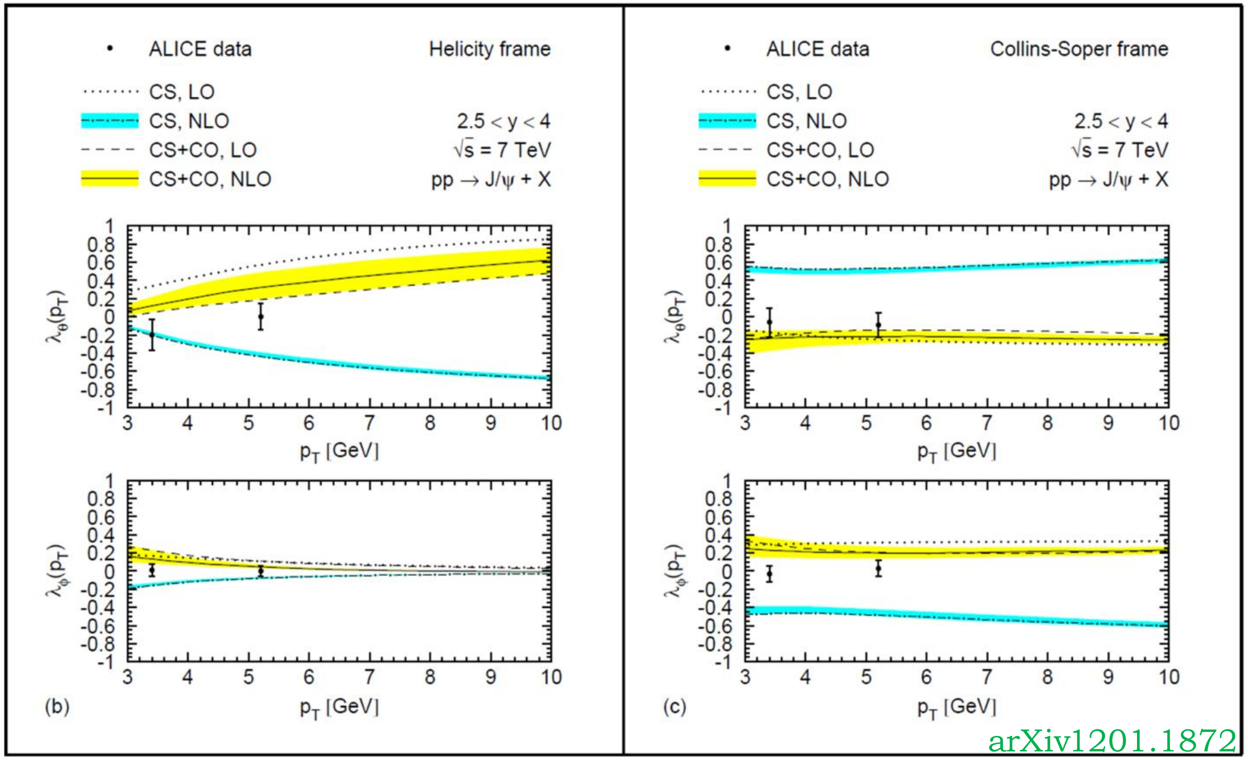

None of the models can perfectly describe the experimental results.

However, NRQCD is slightly favored.

D mesons vs multiplicty

Contribution of Multi Parton Interactions at the LHC?

Correlation between D mesons yield and the total charged particle multiplicity

- Linear increase of the yield with the charged particle density.
- Good consistency of the 3 D mesons species.
- No evident p_T dependence within uncertainties.

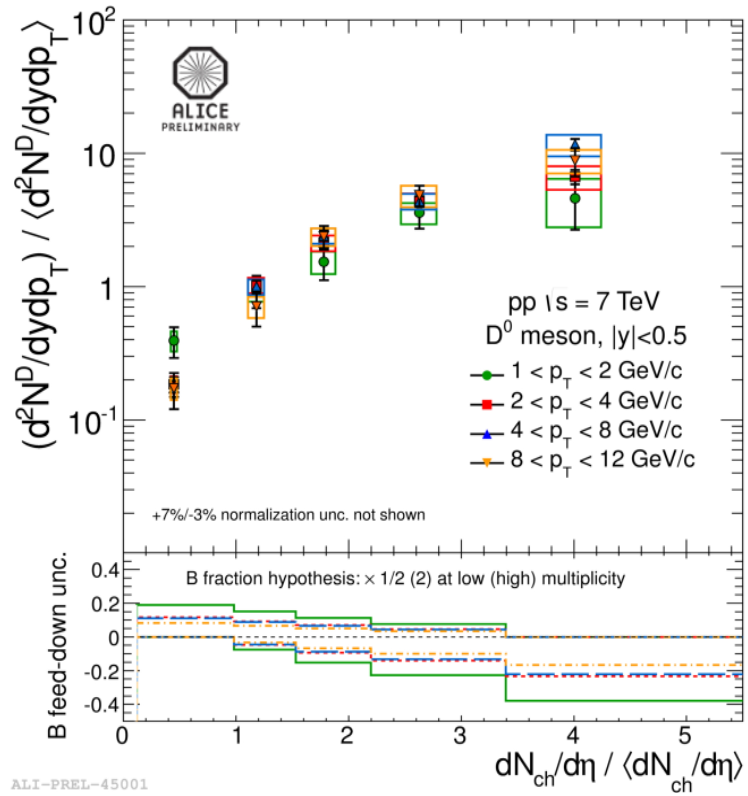

Centrality

The centrality of an event is classified in percentiles of the hadronic cross section using the charged particle multiplicity.

The Anchor Point is defined as the amplitude of the VZERO detector equivalent to 90% of the hadronic cross section.

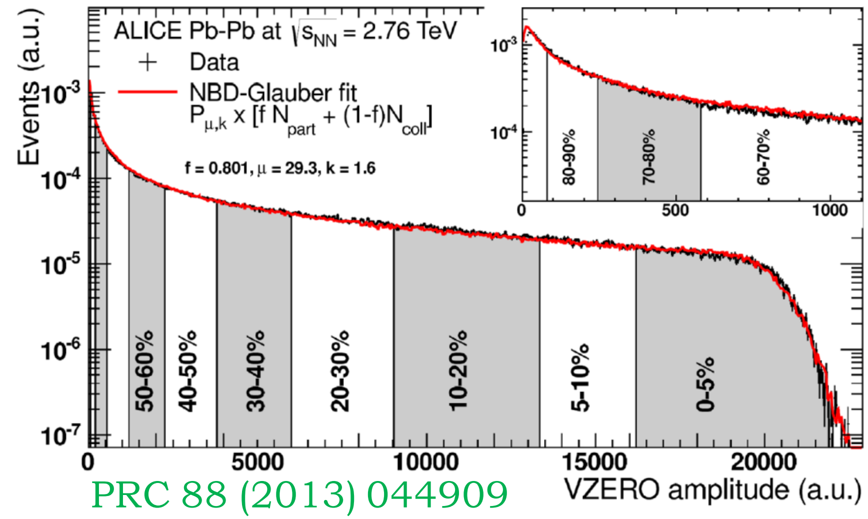

PRC 88 (2013) 044909

The centrality classes correspond to percentiles of the hadronic cross section and are computed via two methods:

1. Using the charged particle multiplicity measured by different detectors with different rapidity coverages (VZERO, SPD and TPC).

2. Measuring the nucleon spectators via the ZDC.